Cell Death and Differentiation (2007) 14, 887–894

www.nature.com/cdd

Review

Constitutive autophagy: vital role in clearance of unfavorable proteins in neurons

M Komatsu[1,2,3], T Ueno[1], S Waguri[4], Y Uchiyama[5], E Kominami[1] and K Tanaka*[,2]

Investigations pursued during the last decade on neurodegenerative diseases have revealed a common mechanism underlying the development of such diseases: conformational disorder of certain proteins leads to the formation of misfolded protein oligomers, which subsequently develop into large protein aggregates. These aggregates entangle other denatured proteins and lipids to form disease-specific inclusion bodies. The failure of the ubiquitin-proteasome system to shred the protein aggregates has led investigators to focus their attention to autophagy, a bulk degradative system coupled with lysosomes, which is involved in non-selective shredding of large amounts of cytoplasmic components. Research in this field has demonstrated the accumulation of autophagic vacuoles and intracytoplasmic protein aggregates in patients with various neurodegenerative diseases. Although autophagy fails to degrade large protein aggregates once they are formed in the cytoplasm, drug-induced activation of autophagy is effective in preventing aggregate deposition, indicating that autophagy significantly contributes to the clearance of aggregate-prone proteins. The pivotal role of autophagy in the clearance of aggregate-prone proteins has been confirmed by a deductive approach using a brain-specific autophagy-ablated mouse model. In this review, we discuss the consequences of autophagy deficiency in neurons.
Cell Death and Differentiation (2007) **14,** 887–894. doi:10.1038/sj.cdd.4402120; published online 2 March 2007

Cell proteins exist in a balance between continuous synthesis and degradation. In general, this flow of synthesis and degradation (i.e., turnover) contributes to exertion of cell-type-specific functions and maintenance of cell homeostasis. However, it is not uncommon that living cells are exposed to various environmental stresses, such as oxygen radicals and UV irradiation. Unfortunately, these stresses frequently cause various types of protein injuries that vitiate normal cellular functions or homeostasis and may eventually cause cell death. Prompt elimination of injured harmful proteins, which is particularly important in non-proliferative cells, such as neurons, is totally dependent on proper function of protein catabolic machineries, in which two major sophisticated apparatuses play principal roles. One is the proteasome, which is an elegantly organized multi-protease complex with catalytic activities inside its central proteinaceous chamber. It plays crucial roles in selective degradation of short-lived regulatory proteins as well as proteins with aberrant structures that should be eliminated from the cells.[1] The other apparatus is the lysosome that contains many acidic hydrolases, which are separated from the cytosol by the limiting membrane. In this lysosomal pathway, degradation of plasma membrane proteins and extracellular proteins is mediated by endocytosis, whereas that of cytoplasmic components is achieved through distinct types of autophagic pathways; for example, macroautophagy, microautophagy, and chaperone-mediated autophagy.[2,3]

Macroautophagy (hereafter referred to as autophagy), the major type of autophagy, is the bulk protein degradation pathway associated with marked membrane dynamics. In response to various stimuli, such as starvation (i.e., nutritional step-down) and humoral (trophic) factors (e.g., glucagon and cytokines), an isolation membrane appears promptly in the cytosol, where it gradually elongates to sequestrate cytoplasmic constituents. Subsequently, the edges of the membrane fuse together to form double-membrane structures termed autophagosomes. Autophagosomes rapidly fuse with lysosomes, and their contents engulfed together with the inner membrane are degraded by a variety of lysosomal digestive hydrolases (Figure 1).[4] In addition to the importance of starvation-induced (i.e., adaptive) autophagy equipped as a fundamental survival strategy in all eukaryotic cells, growing lines of evidence point to the importance of basal autophagy that operates constitutively at low rate even under nutrient-rich environment and to its key role in global turnover of cellular components including organelles.

[1]Department of Biochemistry, Juntendo University School of Medicine, Tokyo, Japan; [2]Laboratory of Frontier Science, Tokyo Metropolitan Institute of Medical Science, Tokyo, Japan; [3]PRESTO, Japan Science and Technology Corporation, Kawaguchi, Japan; [4]Department of Anatomy and Histology, Fukushima Medical University School of Medicine, Fukushima, Japan and [5]Department of Cell Biology and Neurosciences, Osaka University Graduate School of Medicine, Osaka, Japan
*Corresponding author: K Tanaka, Laboratory of Frontier Science, Tokyo Metropolitan Institute of Medical Science, Bunkyo-ku, Tokyo 113-8613, Japan.
Tel/Fax: +81 3 3823 2237; E-mail: tanakak@rinshoken.or.jp
Keywords: autophagy; neurodegenerative diseases; ubiquitin; knockout-mice; Atg7
Abbreviations: AD, Alzheimer's disease; APP, amyloid precursor protein; Aβ, beta-amyloid; GFP, green fluorescent protein; HD, Huntington's disease; LC3, microtubule-associated protein 1 light chain 3/MAP1LC3; mTor, mammalian target of rapamycin; PD, Parkinson's disease; PS1, presenilin-1; SDH, succinate dehydrogenase; TCA, tricarboxylic acid
Received 28.11.06; revised 05.2.07; accepted 05.2.07; Edited by E Baehrecke; published online 02.3.07

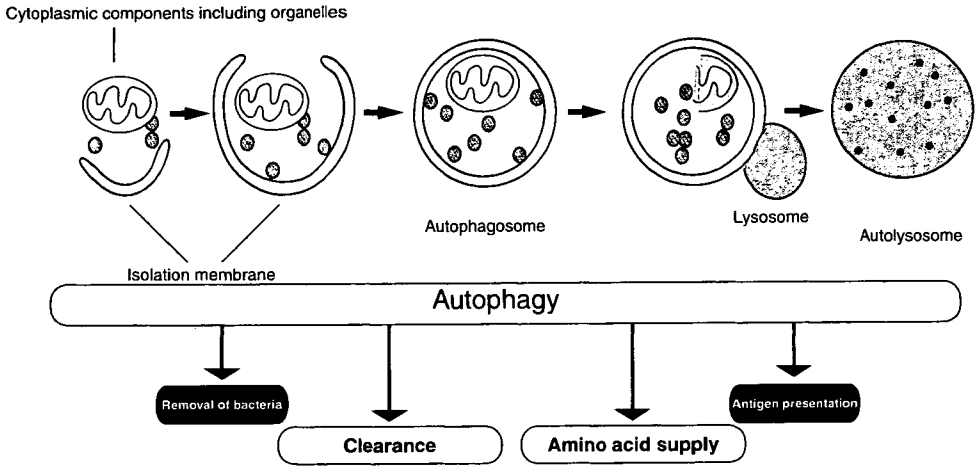

Figure 1 Schematic representation of the physiological functions of autophagy. Autophagy is induced in response to emergency states such as nutrient starvation or bacterial infection, which results in the degradation of cytoplasmic components for amino-acid supply (non-selective process) and the removal of bacteria that invade the cytoplasm (selective process). Autophagy also contributes to processing viral proteins such as EBNA1 and certain cytosolic proteins (e.g., tumor antigens) for presentation onto major histocompatibility complex (MHC) class II molecules. Autophagy also occurs constitutively even under a nutrient-rich state and contributes to global turnover of cellular components. It is an essential cellular process that maintains homeostasis in quiescent cells (e.g., hepatocytes and neurons)

Starvation-induced Autophagy

The most fundamental function of autophagy is cellular adaptation to nutritional stress. In yeast, autophagy is promptly induced upon nitrogen starvation.[5] Transgenic mice overexpressing GFP (green fluorescent protein)-LC3 is an interesting animal model for monitoring autophagy.[6] LC3 (microtubule-associated protein 1 light chain 3/MAP1LC3), originally identified as a small subunit of MAP-1A/MAP-1B, is processed by Atg4B protease to expose the carboxyl-terminal glycine whose residue serves as a donor site for conjugation of target molecules.[7–9] The processed form (LC3-I) undergoes two consecutive ubiquitylation-like modification reactions catalyzed by Atg7 (E1, activating-like enzyme) and Atg3 (E2, conjugating-like enzyme), to be covalently coupled with phosphatidylethanolamine (PE).[10–12] The PE-conjugated form, designated as LC3-II, is then recruited to autophagosomal membrane. Thus, LC3-II is a promising marker for autophagosomal membranes.[7] Similar to endogenous LC3, GFP-LC3 responds to nutrient-starved conditions to form GFP-LC3-II, which is recruited to autophagosomes in GFP-LC3 transgenic mice.[6] The autophagosomal GFP-LC3-II could be detected as dots in fluorescence microscopic analyses. Under fasting conditions, the numbers of fluorescent dots increase in the cytoplasm of the liver, heart, and skeletal muscles of GFP-LC3 transgenic mice.

Starvation-induced protein degradation has been best investigated in the liver. One unequivocal characteristic of hepatic protein degradation is its dependence on the nutrient conditions. Depending on the dietary cycle of the animal, the rate of protein degradation fluctuates between ~1.5% (fed state) and ~4.5% (fasted state) of total liver proteins per hour.[13] Recently, we generated *Atg7*$^{F/F}$:Mx1 mice in which autophagy could be successfully inactivated in the livers.[14] Whereas the amount of total liver proteins decreased to about 66% in the control liver by 1-day fasting, fasting did not result in a significant decrease in the amount of total proteins in the autophagy-deficient liver, indicating that the decrease in total proteins upon fasting is indeed dependent on autophagy. Measurement of the activity of mitochondrial enzyme, succinate dehydrogenase (SDH), showed that fasting was also associated with a significant decrease in SDH activity in total extracts in the control livers, and such reduction was proportional with the decrease in the amount of total protein. On the other hand, fasting was not associated with any change in SDH activity in the autophagy-deficient livers. These results suggest that the mitochondria and cytoplasmic proteins are proportionally degraded upon fasting by autophagy. Thus, it is plausible that autophagosomes surround cytoplasmic components including mitochondria at random to adapt for starvation.

Yeast deficient in autophagy rapidly dies under nutrition-poor conditions,[15] suggesting the important roles of autophagy in maintaining nutrient supply. Indeed, newborn mice deficient in Atg5 or Atg7, which are indispensable for autophagosome formation, show poor response to starvation with regard to production of amino acids, and die within the first day of life.[14,16] Furthermore, Lum *et al.*[17] reported that in IL-3-dependent cells, which cannot undergo apoptosis due to knockout of both Bax and Bak, impairment of autophagy leads to rapid cell death by loss of IL-3, and such death is suppressed by addition of methylpyruvate, a TCA (tricarboxylic acid) substrate. These results suggest that one of the important roles of autophagy is the supply of amino acids under nutrient-poor environment (Figure 2, top panel).

Unique Features of Neuronal Autophagy

The brain appears to be a specially protected tissue where nutrients (e.g., amino acids, glucose, and ketone bodies) are compensated by constant supply from other organs even under starvation conditions and consequently autophagy does not operate in response to nutritional stress. Indeed, autophagosomes-related GFP-LC3 dots do not increase at all

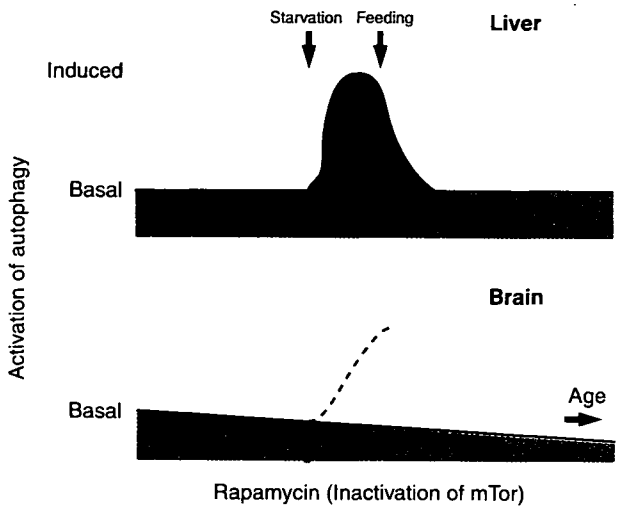

Figure 2 Schematic presentation of induced autophagy and basal (constitutive) autophagy. Under nutrient-rich conditions, autophagic proteolysis proceeds in hepatocytes at a basal rate (top panel, pink zone), which is enhanced two- to threefold to an induced rate under nutrient-starvation conditions (blue zone). When animals are re-fed, the rate of autophagic proteolysis promptly returns to the basal level. In contrast to the liver, autophagy in the brain is thought to proceed at a basal rate, irrespective of nutrient conditions. However, this basal or constitutive autophagy plays a critical role in the quality control system of neurons. Rapamycin and its homologs, which upregulate autophagy to an induced level (bottom panel, broken line), are expected to prevent the accumulation of aggregate-prone proteins. It should be noted that autophagic activity declines with age, which may relate to the age-dependent onset of neurodegenerative diseases

in the brain of GFP-LC3 transgenic mice, irrespective of fasting.[6] A reasonable conclusion drawn from these observations is that autophagy in the brain proceeds at a basal rate but is not enhanced under fasting conditions (Figure 2, bottom panel). Another peculiar feature of autophagy in neurons is the free localization of autophagosomes in the cytoplasm but the restriction of lysosomes mainly to the juxtanuclear cytoplasm of the cell body in the neuron. This feature means that autophagosomes formed in dendrites and synaptic terminal regions must be transported to the lysosome in the cell body. A previous kinetic analysis of organelle movements in cultured neurons indicated that phase-dense vesicles, containing sequestered cytoplasmic proteins and materials taken up by endocytosis, move along microtubules in the axon to the lysosomes in the cell body.[18] These data suggest that fusion of autophagosomes formed in the synaptic cytoplasm with lysosomes is strictly dependent on retrograde axonal transport. It has been reported that mutations of dynein and dynactin in mice and human cause motor neuron degeneration resembling amyotrophic lateral sclerosis.[19,20] Using cultured PC12 cells, flies and mice expressing different kinds of aggregate-prone proteins, such as expanded polyQ and mutant α-synuclein, Ravikumar *et al*.[21] demonstrated that inhibition of dynein function retarded the clearance of aggregates by inhibiting autophagosome-lysosome fusion. It has been shown recently that aggregate-prone proteins formed in the cytoplasm of cultured HeLa cells and a cultured neural cell line, are degraded by autophagy, which is also dependent on intact microtubules.[22]

Autophagic Vacuoles in Neurodegenerative Diseases

Morphological analyses revealed that accumulation of abnormally large number of autophagic vacuoles (autophagosomes plus autolysosomes) or the appearance of irregularly shaped autophagic vacuoles is frequently observed as a common feature in many inherited neurodegenerative diseases.[23–27] Inclusion bodies, composed of ubiquitin-positive cytoplasmic remnants, and lipofuscin deposits, together with dispersed autophagic vacuoles and lysosomes are the primary hallmarks of the late stages of these diseases. Increased density of autophagic vacuoles seems to reflect enhanced autophagosome formation, on one hand, but their accumulation with blurred structures of sequestered materials in their lumen may also imply impaired autolysosomal degradation, on the other. In fact, these morphological features are not present in normal neurons and resemble those of cultured HEK293 cells that have been placed under starvation conditions in the presence of lysosomal proteinase inhibitors.[28] Under these conditions, autophagic response is markedly enhanced, but autophagic proteolysis is simultaneously inhibited. In addition, as observed in Danon disease, which is caused by mutation of the lysosome-associated membrane protein-2 (LAMP-2), and LAMP-2-deficient mice, impairment of autophagosome-lysosome fusion also leads to unequivocal increment of autophagosomes in cardiac muscles and hepatocytes.[29,30]

Autophagy in Alzheimer's, Huntington's, and Parkinson's Diseases

Protein conformational disorders, such as Alzheimer's disease (AD), Huntington's disease (HD), and Parkinson's disease (PD), are characterized by abnormally high accumulation of misfolded and/or unfolded proteins in the surviving neurons as detected at postmortem examination. In this section, we will evaluate the role of autophagy in those hereditary neurodegenerative diseases.

It has become clear that autophagy is linked to the pathogenesis of HD. HD is an autosomal dominant disorder caused by mutations of huntingtin, a cytosolic protein that has a polyglutamine (polyQ) tract in its N-terminus. In HD, abnormal expansion of polyQ caused by codon (CAG) reiterations in exon 1 of the Huntingtin gene produces mutated huntingtin with an expanded polyQ repeat (more than 37 polyQs). Mutant huntingtin with a longer polyQ tract has a stronger tendency than the wild type to form aggregates, both accelerating the onset and worsening the severity of the disease, suggesting that the progressive formation of insoluble polyQ aggregates is a key event leading to manifestation of the disease. Indeed, model mouse with mutant polyQ is associated with formation of nuclear and cytoplasmic inclusions in their neurons.[31] However, recent studies revealed that globular and protofibrillar intermediates form before the organization of mature huntingtin aggregates, and that these are toxic and could lead to disturbances of genetic transcription networks and mitochondrial dysfunctions.[32,33] Then, what are the mechanisms by which autophagy clears mutant huntingtin? Ultrastructural examination of huntingtin-transfected cells showed abundant accumulation of cathepsin

D-positive autophagic vacuoles with or without sequestered cellular constituents, dense lysosomes, and multilamellar and tubuloveseicular structures.[26] Ravikumar *et al.*[34] investigated whether autophagy can degrade mutant huntingtin with expanded polyQ repeats. Degradation of 74 polyQ repeats fused to the amino terminus of GFP (polyQ74-GFP) transfected into COS7 or PC12 cells was inhibited by 3-methyladenine, a specific inhibitor of autophagy, and enhanced by rapamycin. Rapamycin acts by inhibiting the mammalian target of rapamycin (mTor) kinase, which forms the core of a nutrient- and growth factor-sensitive complex that control protein synthesis, and suppresses autophagy.[35] Importantly, inhibitors of autophagy enhance cell death, whereas rapamycin prevents the effects. Furthermore, once the overexpressed polyQ74-GFP forms insoluble large aggregates, the insoluble aggregates become resistant to rapamycin-induced autophagy. The data clearly demonstrate that failure to degrade polyQ expansions by autophagy is associated with accelerated progression of HD and that stimulation of autophagy in the early stages of the disease by rapamycin treatment could prevent deposition of polyQ aggregates. Rapamycin enhances the autophagic clearance of different proteins with long polyQ and polyalanine (polyA)-expanded proteins, and reduces their neurotoxicity. Thus, rapamycin and its analogs can be potentially used therapeutically for neurodegenerative diseases caused by aggregate-prone proteins.[36] It has been shown that mTor is sequestered in polyQ aggregates in transgenic mice expressing mutant huntingtin and patient brains of HD. Sequestration of mTor in polyQ aggregates inhibits nuclear-cytoplasm shuttling of mTor, leading to inactivation of mTor.[37] The inactivation in turn induces autophagy. Hence, co-sequestration of aggregates with mTor leads to inhibition of mTor activity, which may provide a partial explanation for accumulation of autophagic vacuoles in neurodegenerative diseases. On the other hand, the activation of autophagy via an insulin signal pathway clears accumulated polyQ proteins independent of mTor, as reported by Yamamoto *et al.*[38] They found that aggregates of mutant huntingtin activate insulin receptor substrate-2 involving the signaling cascades of insulin and insulin-like growth factor 1. Such activation turns on class III PI3K to induce autophagy, thus contributing to clearance of huntingtin aggregates.[38]

Invariably, AD is the most prevalent form of neurodegenerative diseases with dementia and associates with extracellular deposition of beta-amyloid (Aβ). Presenilin-1 (PS1) is one of several proteins linked to early-onset familial AD, and together with PS2, plays a catalytic role in the γ-secretase complex necessary for intermediate proteolysis of the amyloid precursor protein (APP) followed by liberation of Aβ. Although it has been noticed that autophagic vacuoles accumulate in hippocampal and prefrontal cortical pyramidal neurons of Alzheimer-type dementia,[23,24] the mechanism remains unclear. Wilson *et al.*[39] found the formation of enlarged late endosome-like structures, including α- and β-synuclein, in the perikarya of PS1$^{-/-}$ primary neurons and hippocampal tissue of patients with the Levy body variant of AD. Formation of such organelles is rescued by exogenous expression of not only wild-type PS but also dominant-negative PS1 lacking its activity, indicating that PS1 has another function besides γ-secretase. Esselens *et al.*[40] demonstrated the accumulation of telencephalin, a neural specific intercellular adhesion molecule known to interact with PS1, in vacuoles positive for Atg12 and LC3, but not cathepsin D, in PS1$^{-/-}$ hippocampal neurons. Similar to the report of Wilson *et al*,[39] the formation of such vacuoles was suppressed by not only wild-type but also mutant PS1. Furthermore, Esselens *et al.*[40] used cathepsin D knockout mice to show the degradation of telencephalin in lysosomes. Collectively, these results suggest that PS1 might play important roles in autophagosome and lysosomal fusion step. Recently, Yu *et al.*[41] reported the role of autophagy in Aβ production. Their exhaustive electron and immunoelectron microscopic analyses revealed accumulation of LC3-positive autophagic vacuoles in brains of AD patients and in AD model mice, neural cell lines, and in a non-neural APP-expressing cell line, and also the localization of PS1, Aβ40, Aβ42, and necastrin on internal and limiting membrane components of autophagic vacuoles. Further, they found that induction of autophagy evoked Aβ production, and inversely, inhibition of autophagy suppressed Aβ production. Finally, they observed the PS1-dependent γ-secretase activity in biochemical isolated autophagic vacuoles. Based on these findings, they proposed a novel mechanism for the generation of Aβ via autophagy that emphasized the prominent role of autophagy in AD pathogenesis.[41]

PD is a neurodegenerative disorder associated with progressive loss of dopaminergic neurons of the substantia nigra and locus coeruleus. The major clinical symptoms of PD are body rigidity, hypokinesia, and postural instability associated with trembling extremities.[42] Pathological examination shows marked accumulation of cytoplasmic inclusions of proteinaceous material with lipids called Lewy bodies. Lewy bodies consist of lipids, ubiquitin, enzymes involved in ubiquitin-related pathways, neurofilament proteins, α-synuclein, synphilin-1, and other entangled proteins. Mutations in the gene encoding α-synuclein, which is localized in presynaptic terminals and is abundantly present in Lewy bodies, are identified in certain cases of familial PD.[43,44] α-Synuclein is a protein of unknown function and a major component of Lewy bodies. Among three point mutations in α-synuclein causing an autosomal dominant form of familial PD, two mutations of α-synuclein (A53T and A30P) have been studied extensively. These α-synuclein mutants have a stronger tendency to form fibrils than wild-type α-synuclein. Hence, similar to huntingtin with abnormal polyQ expansion, misfolded or aggregated α-synuclein is believed to cause cell toxicity and inhibits the ubiquitin-proteasome system. Lewy bodies may contribute to aggregation of α-synuclein into inclusions to moderate its toxicity.[45,46] It has been reported recently that autophagic-lysosomal dysfunction may be also involved in PD. Using stable PC12 transfectants expressing wild-type and A53T mutant α-synuclein, Stefanis *et al.*[47] showed that marked accumulation of autophagic vacuoles and impairment of lysosomal and ubiquitin-proteasome functions are principal phenotypes in the cells. On the other hand, clearance of mutant α-synuclein is strongly dependent on both ubiquitin-proteasomes and macroautophagy,[48] but not chaperone-mediated autophagy capable of degrading wild-type α-synuclein efficiently.[49]

Impairment of Autophagy in Neurons

Recently, our group and Mizushima's group investigated the pathophysiological roles of basal or constitutive autophagy in the brain.[50,51] For this purpose, we generated neuron-specific autophagy-deficient mice (*Atg7*$^{F/F}$:Nes mice) by crossing *Atg7*-conditional knockout mice (*Atg7*$^{F/F}$) with transgenic mice expressing the Cre recombinase under the control of the neuron-specific Nestin (Nes) promoter, Nes-*Cre*. We found that mice lacking Atg7 (i.e., autophagy) in the central nervous system exhibited various behavioral deficits, such as abnormal limb-clasping reflexes and reduction of coordinated movement, and died within 28 weeks after birth. Histological analysis showed that *Atg7*-deficiency was associated with neuronal loss in the cerebral and cerebellar cortices. Intriguingly, *Atg7*-deficient neurons showed abundant accumulation of polyubiquitylated proteins, which appeared as inclusion bodies whose size and number increased with aging (Figure 3), but had functionally intact proteasomes, whose impairment is generally known to cause abnormal ubiquitin-mediated proteolysis.[50] Hara *et al.*[51] also reported that almost all these phenotypes, if not all, were observed in neural-specific mice deficient in *Atg5*, another autophagy-essential gene. Thus, many of the critical symptoms seen in neural-specific autophagy-deficient mice are similar to those of patients with neurodegenerative disorders.

Histological analyses of the brains of *Atg7*$^{F/F}$:Nes mice revealed loss of specific neurons, such as pyramidal neurons in the cerebral cortex and hippocampus, and Purkinje cells in the cerebellum. Unexpectedly, immunohistological analysis using anti-ubiquitin antibody identified ubiquitin-positive proteinaceous aggregates throughout the brain, although the staining intensity varied from one region to another. Few ubiquitin-positive inclusions were recognized in brain regions with evident neuronal loss, whereas many ubiquitin inclusions were noted in areas with barely any neuronal loss such as the hypothalamus. Although we could not determine whether neuronal death is due to accumulation and subsequent inclusion formation of ubiquitylated proteins, neurons with large inclusions survived. Conversely, large pyramidal neurons and Purkinje cells seem vulnerable to ubiquitylated proteins and die before the formation of large inclusions. Whether the formation of inclusion bodies in neurons is protective or toxic is under debate, although emerging evidence emphasizes that protein aggregation can be a protective mechanism.[32,33]

Although accumulation of ubiquitylated proteins and cell death were noted in autophagy-deficient hepatocytes[14] and neurons,[50,51] such phenotypes were not observed in growing cells such as mouse embryonic fibroblasts (MEFs) and astroglial cells, irrespective of autophagy deficiency. Thus, it seems that autophagy is not required in rapidly dividing cells, at least with respect to multiplication of these cells. These results might also reflect the difference in autophagic activity among cell types. It is possible that the cell division cycle results in dilution of ubiquitylated proteins in autophagy-deficient MEFs, preventing their accumulation. Alternatively, other degradation pathways, such as chaperone-mediated autophagy, could contribute to degradation of long-lived proteins in growing MEFs. Considered together, it is clear that macroautophagy (the massive autophagy pathway discussed here) plays important roles in proteolysis in quiescent cells.

Autophagy deficiency is considered to result in delays of global turnover of cytoplasmic components, resulting in accumulation of misfolded and/or unfolded proteins followed by formation of inclusion bodies. However, a recent report showed that p62/SQSTM1 harboring a ubiquitin binding domain, interacted with LC3 and was degraded via autophagy.[52] We also obtained similar results and found that

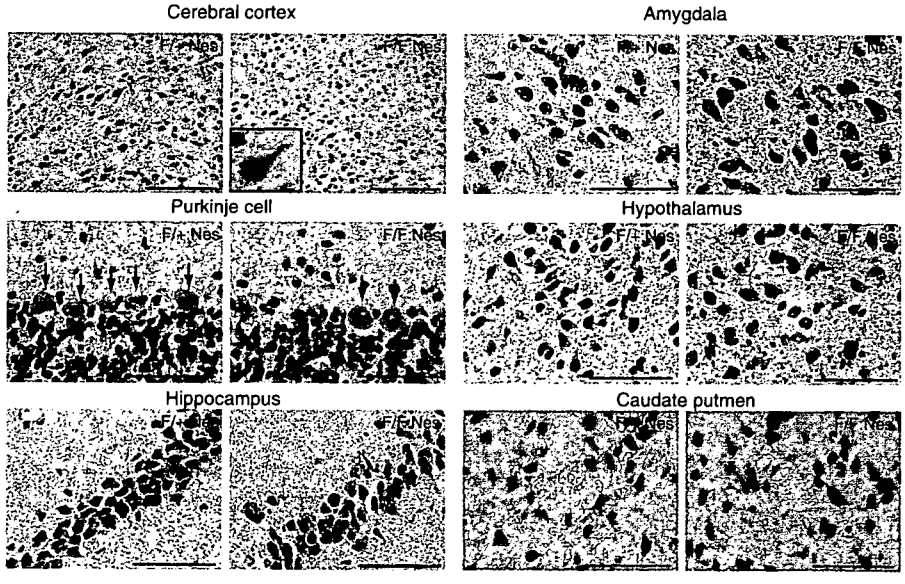

Figure 3 Ubiquitin-positive inclusions in autophagy-deficient neurons. The presence of ubiquitin-positive dots was examined immunohistochemically in several regions of the brain including cerebral cortex, cerebellum (Purkinje cells), hippocampus, amygdala, hypothalamus, caudate putamen of *Atg7*$^{F/+}$:Nes (left panels), and *Atg7*$^{F/F}$:Nes (right panels) mice. Note the presence of numerous ubiquitin dots in the amygdala and hypothalamus of representative mutants. Bars, 100 μm in the panel of cerebral cortex, and 50 μm in others

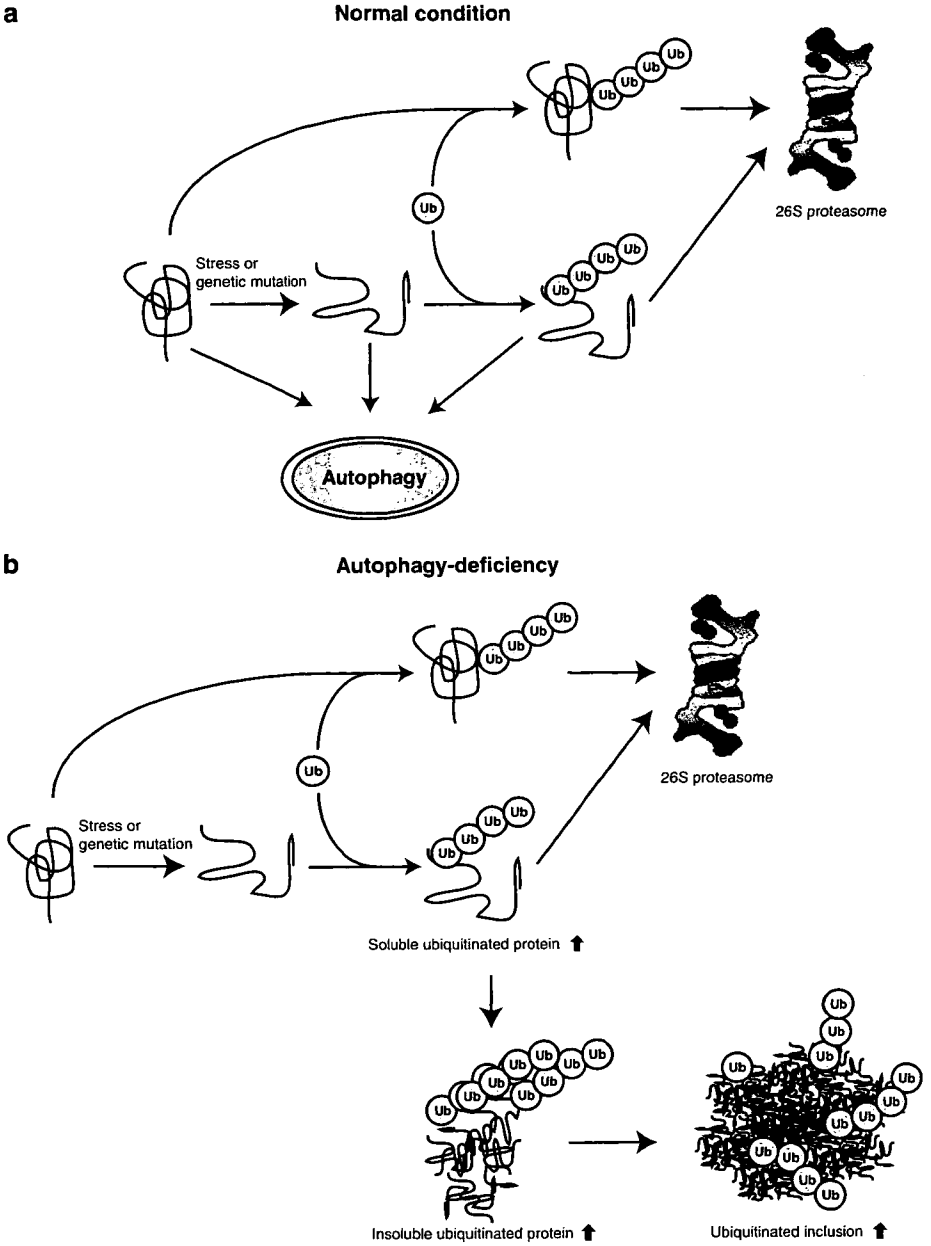

Figure 4 A schematic diagram of protein destruction pathways mediated by the proteasome and autophagy. The majority of cellular proteins, if not all, are polyubiquitylated before hydrolysis by the proteasome (an ATP-dependent proteolytic complex). Similarly, unfolded/misfolded proteins generated by environmental stresses or genetic mutations are discarded after polyubiquitylation by the same proteolytic system (**a**). Aging-related decline in autophagic activity causes accumulation of highly ubiquitylated proteins, which are recovered as both soluble and insoluble forms (**b**). As autophagy could feed both ubiquitylated and unubiquitylated protein(s), it is not clear at present whether polyubiquitylated aggregates/inclusions in autophagy-deficient neurons are formed consequent to impairment of degradation of unubiquitylated proteins or aggressively polyubiquitylated proteins. In addition, further work is needed to determine whether the two proteolytic systems (autophagy and proteasomes) work independently or cooperatively, and whether autophagy and the proteasome feed a similar set of normal and/or misfolded/unfolded proteins in general. Red text: protein dynamics associated with autophagy deficiency, Ub: ubiquitin

p62 plays a critical role in the formation of ubiquitin-positive aggregates by impaired autophagy (unpublished data). These results imply that ubiquitylated unfavorable proteins might be selectively sequestered into autophagosomes in part via p62 (which may retain its shuttling ability of ubiquitylated proteins). In either case (non-selective or selective degradation of ubiquitylated proteins by autophagy), our results indicate that autophagy operates not only as a supplier of amino acids under nutrient-poor conditions but also as a house cleaner of damaged proteins under nutrient-rich conditions.

Concluding Remarks

Considering the role of autophagy in neurodegenerative diseases, it is possible to align time-dependent enhancement and inactivation of autophagy. First, misfolded and/or

unfolded protein aggregates formed in neurons cause sequestration of mTor along with the aggregates, leading to significant inactivation of mTor, which stimulates autophagy (autophagosome formation). Second, if the size of aggregates is small enough and the degree of aggregation is moderate, the aggregates are engulfed into autophagosomal lumen and subsequently degraded via autophagy. Unless the amounts of aggregates surpass the clearance capacity of autophagosomes, maximal activation of autophagy by pharmaceutical agents such as rapamycin could be effective in preventing the progression of the disease. It is noteworthy that the expression of aggregation-prone protein(s) observed frequently in familial neurodegenerative disorders is not required for the formation of inclusions associated with impaired autophagy, suggesting the involvement of autophagy even in sporadic neurodegenerative diseases. On the other hand, autophagic activity of rat liver decreases with aging and this decrease conversely correlates with an increase in the accumulation of oxidized proteins.[36] Thus, age-dependent onset of neurodegenerative diseases most likely correlates with the age-dependent decline of autophagic activity. It is generally accepted that deficits of the proteasome-ubiquitin system are linked to various neurodegenerative disorders. Intriguingly, however, no obvious inhibition of the ubiquitin-proteasome system occurs in the mouse brain lacking autophagy, providing compelling evidence that constitutive autophagy plays a prominent role in neuronal survival, independent of proteasome function (Figure 4). In this context, we stress that proteasome inhibition induces augmented autophagy in order to eliminate unnecessary accumulated proteins, probably compensating the loss of proteasome functions.[22] Thus, the two major proteolytic pathways naturally differ in the cooperative responses in cells. We emphasize the importance of autophagy as a process with adaptive and flexible responses. Finally, a better understanding of basal or constitutive autophagy, which maintains basal activity of macroautophagy in neurons, may help in the design of new strategies to prevent neurodegenerative diseases.

1. Goldberg AL. Protein degradation and protection against misfolded or damaged proteins. *Nature* 2003; **426**: 895–899.
2. Levine B, Klionsky DJ. Development by self-digestion: molecular mechanisms and biological functions of autophagy. *Dev Cell* 2004; **6**: 463–477.
3. Cuervo AM. Autophagy: in sickness and in health. *Trends Cell Biol* 2004; **14**: 70–77.
4. Mizushima N, Ohsumi Y, Yoshimori T. Autophagosome formation in mammalian cells. *Cell Struct Funct* 2002; **27**: 421–429.
5. Takeshige K, Baba M, Tsuboi S, Noda T, Ohsumi Y. Autophagy in yeast demonstrated with proteinase-deficient mutants and conditions for its induction. *J Cell Biol* 1992; **119**: 301–311.
6. Mizushima N, Yamamoto A, Matsui M, Yoshimori T, Ohsumi Y. *In vivo* analysis of autophagy in response to nutrient starvation using transgenic mice expressing a fluorescent autophagosome marker. *Mol Biol Cell* 2004; **15**: 1101–1111.
7. Kabeya Y, Mizushima N, Ueno T, Yamamoto A, Kirisako T, Noda T *et al.* LC3, a mammalian homologue of yeast Apg8p, is localized in autophagosome membranes after processing. *EMBO J* 2000; **19**: 5720–5728.
8. Kabeya Y, Mizushima N, Yamamoto A, Oshitani-Okamoto S, Ohsumi Y, Yoshimori T. LC3, GABARAP and GATE16 localize to autophagosomal membrane depending on form-II formation. *J Cell Sci* 2004; **117**: 2805–2812.
9. Tanida I, Sou YS, Ezaki J, Minematsu-Ikeguchi N, Ueno T, Kominami E. HsAtg4B/HsApg4B/autophagin-1 cleaves the carboxyl termini of three human Atg8 homologues and delipidates microtubule-associated protein light chain 3- and GABAA receptor-associated protein-phospholipid conjugates. *J Biol Chem* 2004; **279**: 36268–36276.
10. Ichimura Y, Kirisako T, Takao T, Satomi Y, Shimonishi Y, Ishihara N *et al.* A ubiquitin-like system mediates protein lipidation. *Nature* 2000; **408**: 488–492.
11. Tanida I, Tanida-Miyake E, Ueno T, Kominami E. The human homolog of Saccharomyces cerevisiae Apg7p is a Protein-activating enzyme for multiple substrates including human Apg12p, GATE-16, GABARAP, and MAP-LC3. *J Biol Chem* 2001; **276**: 1701–1706.
12. Tanida I, Tanida-Miyake E, Komatsu M, Ueno T, Kominami E. Human Apg3p/Aut1p homologue is an authentic E2 enzyme for multiple substrates, GATE-16, GABARAP, and MAP-LC3, and facilitates the conjugation of hApg12p to hApg5p. *J Biol Chem* 2002; **277**: 13739–13744.
13. Mortimore GE, Hutson NJ, Surmacz CA. Quantitative correlation between proteolysis and macro- and microautophagy in mouse hepatocytes during starvation and refeeding. *Proc Natl Acad Sci USA* 1993; **80**: 2179–2183.
14. Komatsu M, Waguri S, Ueno T, Iwata J, Murata S, Tanida I *et al.* Impairment of starvation-induced and constitutive autophagy in Atg7-deficient mice. *J Cell Biol* 2005; **169**: 425–434.
15. Tsukada M, Ohsumi Y. Isolation and characterization of autophagy-defective mutants of Saccharomyces cerevisiae. *FEBS Lett* 1993; **333**: 169–174.
16. Kuma A, Hatano M, Matsui M, Yamamoto A, Nakaya H, Yoshimori T *et al.* The role of autophagy during the early neonatal starvation period. *Nature* 2004; **432**: 1032–1036.
17. Lum JJ, Bauer DE, Kong M, Harris MH, Li C, Lindsten T *et al.* Growth factor regulation of autophagy and cell survival in the absence of apoptosis. *Cell* 2005; **120**: 237–248.
18. Hollenbeck PJ. Products of endocytosis and autophagy are retrieved from axons by regulated retrograde organelle transport. *J Cell Biol* 1993; **121**: 305–315.
19. Puls I, Jonnakuty C, LaMonte BH, Holzbaur EL, Tokito M, Mann E *et al.* Mutant dynactin in motor neuron disease. *Nat Genet* 2003; **33**: 455–456.
20. Hafezparast M, Klocke R, Ruhrberg C, Marquardt A, Ahmad-Annuar A, Bowen S *et al.* Mutations in dynein link motor neuron degeneration to defects in retrograde transport. *Science* 2003; **300**: 808–812.
21. Ravikumar B, Acevedo-Arozena A, Imarisio S, Berger Z, Vacher C, O'Kane CJ *et al.* Dynein mutations impair autophagic clearance of aggregate-prone proteins. *Nat Genet* 2005; **37**: 771–776.
22. Iwata A, Riley BE, Johnston JA, Kopito RR. HDAC6 and microtubules are required for autophagic degradation of aggregated huntingtin. *J Biol Chem* 2005; **280**: 40282–40292.
23. Okamoto K, Hirai S, Iizuka T, Yanagisawa T, Watanabe M. Reexamination of granulovacuolar degeneration. *Acta Neuropathol (Berlin)* 1991; **82**: 340–345.
24. Cataldo AM, Hamilton DJ, Barnett JL, Paskevich PA, Nixon RA. Properties of the endosomal-lysosomal system in the human central nervous system: disturbances mark most neurons in populations at risk to degenerate in Alzheimer's disease. *J Neurosci* 1996; **16**: 186–199.
25. Anglade P, Vyas S, Javoy-Agid F, Herrero MT, Michel PP, Marquez J *et al.* Apoptosis and autophagy in nigral neurons of patients with Parkinson's disease. *Histol Histopathol* 1997; **12**: 25–31.
26. Kegel KB, Kim M, Sapp E, McIntyre C, Castano JG, Aronin N *et al.* Huntingtin expression stimulates endosomal-lysosomal activity, endosome tubulation, and autophagy. *J Neurosci* 2000; **20**: 7268–7278.
27. Petersen A, Larsen KE, Behr GG, Romero N, Przedborski S, Brundin P *et al.* Expanded CAG repeats in exon 1 of the Huntington's disease gene stimulate dopamine-mediated striatal neuron autophagy and degeneration. *Hum Mol Genet* 2001; **10**: 1243–1254.
28. Tanida I, Minematsu-Ikeguchi N, Ueno T, Kominami E. Lysosomal turnover, but not a cellular level, of endogenous LC3 is a marker for autophagy. *Autophagy* 2005; **1**: 84–91.
29. Nishino I, Fu J, Tanji K, Yamada T, Shimojo S, Koori T *et al.* Primary LAMP-2 deficiency causes X-linked vacuolar cardiomyopathy and myopathy (Danon disease). *Nature* 2000; **406**: 906–910.
30. Tanaka Y, Guhde G, Suter A, Eskelinen EL, Hartmann D, Lullmann-Rauch R *et al.* Accumulation of autophagic vacuoles and cardiomyopathy in LAMP-2-deficient mice. *Nature* 2000; **406**: 902–906.
31. Ikeda H, Yamaguchi M, Sugai S, Aze Y, Narumiya S, Kakizuka A. Expanded polyglutamine in the Machado–Joseph disease protein induces cell death *in vitro* and *in vivo*. *Nat Genet* 1996; **13**: 196–202.
32. Sanchez I, Mahlke C, Yuan J. Pivotal role of oligomerization in expanded polyglutamine neurodegenerative disorders. *Nature* 2003; **421**: 373–379.
33. Arrasate M, Mitra S, Schweitzer ES, Segal MR, Finkbeiner S. Inclusion body formation reduces levels of mutant huntingtin and the risk of neuronal death. *Nature* 2004; **431**: 805–810.
34. Ravikumar B, Duden R, Rubinsztein DC. Aggregate-prone proteins with polyglutamine and polyalanine expansions are degraded by autophagy. *Hum Mol Genet* 2002; **11**: 1107–1117.
35. Inoki K, Corradetti MN, Guan KL. Dysregulation of the TSC-mTOR pathway in human disease. *Nat Genet* 2005; **37**: 19–24.
36. Bergamini E. Autophagy: a cell repair mechanism that retards ageing and age-associated diseases and can be intensified pharmacologically. *Mol Aspects Med* 2006; **27**: 403–410.
37. Ravikumar B, Vacher C, Berger Z, Davies JE, Luo S, Oroz LG *et al.* Inhibition of mTOR induces autophagy and reduces toxicity of polyglutamine expansions in fly and mouse models of Huntington disease. *Nat Genet* 2004; **36**: 585–595.
38. Yamamoto A, Cremona ML, Rothman JE. Autophagy-mediated clearance of huntingtin aggregates triggered by the insulin-signaling pathway. *J Cell Biol* 2006; **172**: 719–731.
39. Wilson CA, Murphy DD, Giasson BI, Zhang B, Trojanowski JQ, Lee VM. Degradative organelles containing mislocalized alpha-and beta-synuclein proliferate in presenilin-1 null neurons. *J Cell Biol* 2004; **165**: 335–346.

40. Esselens C, Oorschot V, Baert V, Raemaekers T, Spittaels K, Serneels L *et al.* Presenilin 1 mediates the turnover of telencephalin in hippocampal neurons via an autophagic degradative pathway. *J Cell Biol* 2004; **166**: 1041–1054.
41. Yu WH, Cuervo AM, Kumar A, Peterhoff CM, Schmidt SD, Lee JH *et al.* Macroautophagy – a novel Beta-amyloid peptide-generating pathway activated in Alzheimer's disease. *J Cell Biol* 2005; **171**: 87–98.
42. Jenner P, Olanow CW. Understanding cell death in Parkinson's disease. *Ann Neurol* 1998; **44**: S72–S84.
43. Kruger R, Kuhn W, Muller T, Woitalla D, Graeber M, Kosel S *et al.* Ala30Pro mutation in the gene encoding alpha-synuclein in Parkinson's disease. *Nat Genet* 1998; **18**: 106–108.
44. Polymeropoulos MH, Lavedan C, Leroy E, Ide SE, Dehejia A, Dutra A *et al.* Mutation in the alpha-synuclein gene identified in families with Parkinson's disease. *Science* 1997; **276**: 2045–2047.
45. Chung KK, Dawson VL, Dawson TM. The role of the ubiquitin-proteasomal pathway in Parkinson's disease and other neurodegenerative disorders. *Trends Neurosci* 2001; **24**: S7–S14.
46. Mouradian MM. Recent advances in the genetics and pathogenesis of Parkinson disease. *Neurology* 2002; **58**: 179–185.
47. Stefanis L, Larsen KE, Rideout HJ, Sulzer D, Greene LA. Expression of A53T mutant but not wild-type alpha-synuclein in PC12 cells induces alterations of the ubiquitin-dependent degradation system, loss of dopamine release, and autophagic cell death. *J Neurosci* 2001; **21**: 9549–9560.
48. Webb JL, Ravikumar B, Atkins J, Skepper JN, Rubinsztein DC. Alpha-Synuclein is degraded by both autophagy and the proteasome. *J Biol Chem* 2003; **278**: 25009–25013.
49. Cuervo AM, Stefanis L, Fredenburg R, Lansbury PT, Sulzer D. Impaired degradation of mutant alpha-synuclein by chaperone-mediated autophagy. *Science* 2004; **305**: 1292–1295.
50. Komatsu M, Waguri S, Chiba T, Murata S, Iwata J, Tanida I *et al.* Loss of autophagy in the central nervous system causes neurodegeneration in mice. *Nature* 2006; **441**: 880–884.
51. Hara T, Nakamura K, Matsui M, Yamamoto A, Nakahara Y, Suzuki-Migishima R *et al.* Suppression of basal autophagy in neural cells causes neurodegenerative disease in mice. *Nature* 2006; **441**: 885–889.
52. Bjorkoy G, Lamark T, Brech A, Outzen H, Perander M, Overvatn A *et al.* p62/SQSTM1 forms protein aggregates degraded by autophagy and has a protective effect on huntingtin-induced cell death. *J Cell Biol* 2005; **171**: 603–614.

Molecular Cell
Previews

Unlocking the Proteasome Door

Yasushi Saeki[1] and Keiji Tanaka[1,*]
[1]Laboratory of Frontier Science, Core Technology and Research Center, Tokyo Metropolitan Institute of Medical Science, Bunkyo-ku, Tokyo 113-8613, Japan
*Correspondence: tanakak@rinshoken.or.jp
DOI 10.1016/j.molcel.2007.09.001

How proteasomal ATPases stimulate the gate opening of 20S proteasomes is a longstanding question. In the September 7 issue of *Molecular Cell*, Smith et al. (2007) describe the conserved "HbYX" motif as the key to proteasome gate opening.

The multicatalytic protease complex, the 26S proteasome, is responsible for regulated proteolysis in eukaryotic cells (reviewed in Pickart and Cohen, 2004). The 26S proteasome is composed of catalytic 20S proteasomes (20S CP) and one or two 19S regulatory complexes (19S RP, or PA700) (Figure 1A). The 20S proteasome is a barrel-shaped complex composed of 14 α and 14 β subunits arranged as a cylinder in heteroheptameric rings (i.e., $\alpha_{1-7}\beta_{1-7}\beta_{1-7}\alpha_{1-7}$). The active sites are sequestered within a cavity formed by two inner β rings. Substrates access the catalytic sites only through the central pore in the α rings. Importantly, free 20S proteasomes exist in an autoinhibited state in which the N termini of the α subunits form a gate to block substrate entry. Activation of 20S proteasomes occurs upon opening of this gate by a proteasome activator. To date, three different kinds of proteasome activators have been identified; 19S RP/PA700, PA28 (or PA26)/11S regulator, and PA200. The 19S RP contains six ATPase subunits (Rpt1–6) that are organized in a hexameric ring and facilitate gate opening and substrate unfolding using ATP. PA28 is a ring-shaped, dome-like complex composed of seven small subunits, whereas PA200 is a single 200 kDa molecule folded in a solenoid structure. The latter two activators stimulate 20S proteasomes without ATP.

The mechanism of how PA26 controls the gate opening of 20S proteasomes is well established (Förster et al., 2005). PA26 from *Trypanosoma brucei* is a homoheptameric complex that activates 20S proteasomes. The crystal structure of the PA26-20S proteasome complex shows that PA26 binds to 20S proteasomes by inserting its C termini into the intersubunit pockets between adjacent α subunits. In addition, a distinct domain of PA26, termed the "activation loop," is also required to stabilize the gate-opening conformation. Interestingly, activation of 20S proteasomes by PAN, an archaeal ATPase complex that is related to the 19S ATPases, also requires its C-terminal residues. This finding implies that the mechanism of gate opening by proteasomal ATPases is PA26 related, although the precise mechanism is still largely unknown.

In the September 7 issue of *Molecular Cell*, Smith et al. (2007) describe how proteasomal ATPases associate and stimulate the gate opening of 20S proteasomes. Among the archaeal PAN and three 19S ATPase subunits, they found a conserved three-residue C-terminal motif: hydrophobic-tyrosine-X (HbYX). To uncover the significance of this conserved motif, the authors first used the archaeal 20S proteasome and PAN for simplicity, because the symmetric archaeal 20S proteasome contains just one type of α and one type of β subunit, and PAN is a homoheptamer (Förster et al., 2005; Smith et al., 2005). Mutational analysis of the PAN C-terminal LYR sequence revealed that the hydrophobic residue (Leu) and penultimate Tyr residue were essential for proteasomal activation. While the Arg residue can be substituted by other residues, its enzymatic removal or deletion abolished PAN activity. These PAN mutants could not form the PAN-20S complex, suggesting that the HbYX motif itself could bind intersubunit pockets of the 20S α rings. The results of fluorescence polarization assays using a tryptophan-introduced PAN and the 20S pocket mutant support this idea. To test whether the PAN C termini are sufficient to induce gate opening, a series of PAN C-terminal peptides were assayed. Importantly, the peptides of seven residues or longer stimulated 20S proteasome activity and competed with PAN binding. Thus, the PAN C termini are inserted into the 20S α pockets and autonomously induce the gate opening like a "key in a lock" mechanism as proposed (Smith et al., 2007).

Is the HbYX motif-dependent mechanism conserved in more complex and elaborate 26S proteasomes? Of the six 19S ATPases, only three subunits, Rpt2, Rpt3, and Rpt5, contain the HbYX motif. Earlier studies suggested that the functions of the six 19S ATPases are not similar despite their high sequence homology (Rubin et al., 1998). One ATPase, Rpt2, plays a role in gate opening, while Rpt5 plays a role in ubiquitin-chain recognition (Kohler et al., 2001; Pickart and Cohen, 2004). Furthermore, the gate and intersubunit pockets are not fully conserved in eukaryotic 20S proteasomes. The N termini of only three of seven α subunits form a gate, and the open-gate conformation is rather unstable (Groll et al., 2000). Of the seven possible intersubunit pocket combinations, only five are observed in yeast and six in mammals (Förster et al., 2005).

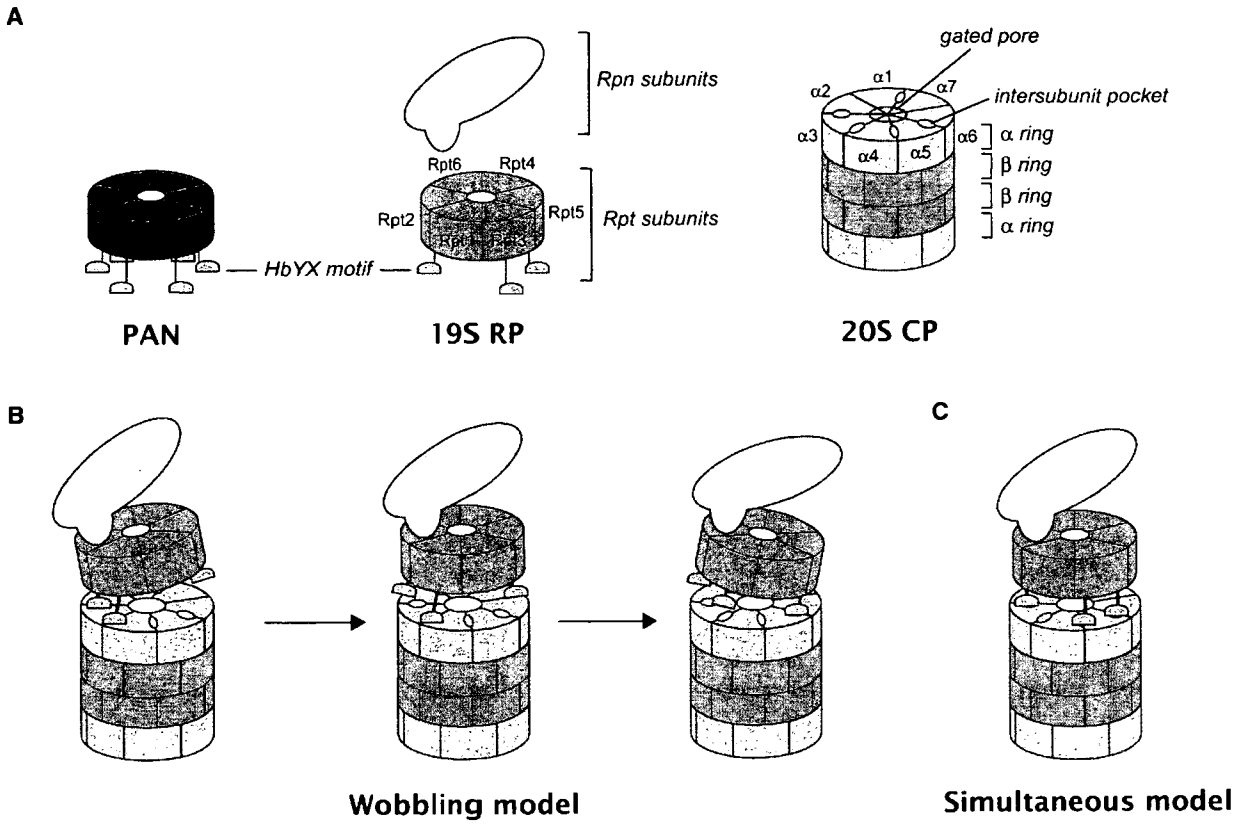

Figure 1. The HbYX Motif of Proteasomal ATPases Functions in the Gate Opening of the 20S Proteasome
(A) Schematic illustrations of the archaeal PAN ATPase complex, eukaryotic 19S RP (consisting of Rpt and Rpn subunits), and 20S proteasomes consisting of α and β rings (i.e., $\alpha_{1-7}\beta_{1-7}\beta_{1-7}\alpha_{1-7}$ complex). The spatial arrangement of the 19S ATPases is depicted according to the subunit interaction map (Fu et al., 2001).
(B) Wobbling model.
(C) Simultaneous model.

To determine the effects of 19S ATPase C termini, all six C-terminal octapeptides from 19S ATPases were synthesized and assayed with mammalian 20S proteasomes. Interestingly, the C-terminal peptides of two subunits, Rpt2 and Rpt5, were able to induce gate opening, while the C-terminal peptide of Rpt3 failed to activate 20S proteasomes. To evaluate the biological significance of the C termini of 19S ATPases, the authors created a series of yeast 26S proteasome mutants, in which the penultimate Tyr was substituted with Ala in each of the different ATPase subunits. Remarkably, studies of affinity-purified proteasomes showed that single point mutations in the HbYX motif of Rpt2, Rpt3, and Rpt5 caused a defect in gate opening but did not affect 19S-20S interaction. Although more systematic in vivo studies of these mutations are being pursued, it is clear at present that multiple HbYX motifs of three subunits specifically facilitate in the gate opening.

One unresolved question is how the ATPase six-fold symmetric ring can associate with the seven-fold symmetric 20S α ring and maintain the open-gate conformation. Like other members of the AAA+ proteins, proteasomal ATPases also undergo conformational changes that are linked to ATP binding and/or hydrolysis in multiple steps upon protein degradation (Ogura and Tanaka, 2003; Hanson and Whiteheart, 2005). Because only two to four subunits of hexameric ATPases are thought to bind ATP simultaneously, not all proteasomal ATPase subunits can engage in gate opening simultaneously. Thus, only a subset of ATPase subunit C termini are inserted into 20S pockets, and this activity may occur sequentially to stabilize the gate-opening state, promoting an apparent "wobbling" of the ATPases on the 20S proteasome (Figure 1B). Alternatively, ATP utilization may differ between subsets of ATPase subunits: e.g., Rpt2 and Rpt5 may always be in an ATP-bound form and stabilize the open-gate conformation, whereas the remaining ATPase subunits may participate in a dynamic ATPase cycle for protein unfolding. In this model, the 26S proteasome is a stable complex and two or three ATPase subunits bind 20S pockets simultaneously to open the gate (Figure 1C). Further studies should elucidate how each proteasomal ATPase subunit utilizes ATP and controls the gate opening upon protein degradation.

REFERENCES

Förster, A., Masters, E.I., Whitby, F.G., Robinson, H., and Hill, C.P. (2005). Mol. Cell *18*, 589–599.

Fu, H., Reis, N., Lee, Y., Glickman, M.H., and Vierstra, R.D. (2001). EMBO J. *20*, 7096–7107.

Groll, M., Bajorek, M., Kohler, A., Moroder, L., Rubin, D.M., Huber, R., Glickman, M.H., and Finley, D. (2000). Nat. Struct. Biol. *7*, 1062–1067.

Hanson, P., and Whiteheart, S.W. (2005). Nat. Rev. Mol. Cell Biol. *6*, 519–529.

Kohler, A., Cascio, P., Leggett, D.S., Woo, K.M., Goldberg, A.L., and Finley, D. (2001). Mol. Cell *7*, 1143–1152.

Ogura, T., and Tanaka, K. (2003). Mol. Cell *11*, 3–5.

Pickart, C.M., and Cohen, R.E. (2004). Nat. Rev. Mol. Cell Biol. *5*, 177–187.

Rubin, D.M., Glickman, M.H., Larsen, C.N., Dhruvakumar, S., and Finley, D. (1998). EMBO J. *17*, 4909–4919.

Smith, D.M., Kafri, G., Cheng, Y., Ng, D., Walz, T., and Goldberg, A.L. (2005). Mol. Cell *20*, 687–698.

Smith, D.M., Chang, S.-C., Park, S., Finley, D., Cheng, Y., and Goldberg, A.L. (2007). Mol. Cell *27*, 731–744.

Schimanski B, Nguyen TN, Günzl A (2005a) Characterization of a multisubunit transcription factor complex essential for spliced-leader RNA gene transcription in *Trypanosoma brucei*. *Mol Cell Biol* **25:** 7303–7313

Schimanski B, Nguyen TN, Günzl A (2005b) Highly efficient tandem affinity purification of trypanosome protein complexes based on a novel epitope combination. *Eukaryot Cell* **4:** 1942–1950

Schnare MN, Gray MW (1999) A candidate U1 small nuclear RNA for trypanosomatid protozoa. *J Biol Chem* **274:** 23691–23694

Schümperli D, Pillai RS (2004) The special Sm core structure of the U7 snRNP: far-reaching significance of a small nuclear ribonucleoprotein. *Cell Mol Life Sci* **61:** 2560–2570

Séraphin B (1995) Sm and Sm-like proteins belong to a large family: identification of proteins of the U6 as well as the U1, U2, U4 and U5 snRNPs. *EMBO J* **14:** 2089–2098

Thompson JD, Higgins DG, Gibson TJ (1994) CLUSTAL W: improving the sensitivity of progressive multiple sequence alignment through sequence weighting, position-specific gap penalties and weight matrix choice. *Nucleic Acids Res* **22:** 4673–4680

Urlaub H, Raker VA, Kostka S, Lührmann R (2001) Sm protein-Sm site RNA interactions within the inner ring of the spliceosomal snRNP core structure. *EMBO J* **20:** 187–196

Will CL, Lührmann R (2001) Spliceosomal UsnRNP biogenesis, structure and function. *Curr Opin Cell Biol* **13:** 290–301

Xu Y, Ben-Shlomo H, Michaeli S (1997) The U5 RNA of trypanosomes deviates from the canonical U5 RNA: the *Leptomonas collosoma* U5 RNA and its coding gene. *Proc Natl Acad Sci USA* **94:** 8473–8478

Yong J, Wan L, Dreyfuss G (2004) Why do cells need an assembly machine for RNA-protein complexes? *Trends Cell Biol* **14:** 226–232

Zaric B, Chami M, Remigy H, Engel A, Ballmer-Hofer K, Winkler FK, Kambach C (2005) Reconstitution of two recombinant LSm protein complexes reveals aspects of their architecture, assembly, and function. *J Biol Chem* **280:** 16066–16075

The EMBO Journal (2006) 25, 4524–4536 | © 2006 European Molecular Biology Organization | All Rights Reserved 0261-4189/06
www.embojournal.org

THE EMBO JOURNAL

A novel proteasome interacting protein recruits the deubiquitinating enzyme UCH37 to 26S proteasomes

Jun Hamazaki[1,2], Shun-ichiro Iemura[3], Tohru Natsume[3], Hideki Yashiroda[1], Keiji Tanaka[1] and Shigeo Murata[1,4,*]

[1]Laboratory of Frontier Science, Core Technology and Research Center, Tokyo Metropolitan Institute of Medical Science, Bunkyko-ku, Tokyo, Japan, [2]Department of Biological Sciences, Graduate School of Science, Tokyo Metropolitan University, Hachiohji, Tokyo, Japan, [3]National Institutes of Advanced Industrial Science and Technology, Biological Information Research Center, Kohtoh-ku, Tokyo, Japan and [4]PRESTO, Japan Science and Technology Agency, Kawaguchi, Saitama, Japan

The 26S proteasome is a multisubunit protease responsible for regulated proteolysis in eukaryotic cells. It is composed of one catalytic 20S proteasome and two 19S regulatory particles attached on both ends of 20S proteasomes. Here, we describe the identification of Adrm1 as a novel proteasome interacting protein in mammalian cells. Although the overall sequence of Adrm1 has weak homology with the yeast Rpn13, the amino- and carboxyl-terminal regions exhibit significant homology. Therefore, we designated it as hRpn13. hRpn13 interacts with a base subunit Rpn2 via its amino-terminus. The majority of 26S proteasomes contain hRpn13, but a portion of them does not, indicating that hRpn13 is not an integral subunit. Intriguingly, we found that hRpn13 recruits UCH37, a deubiquitinating enzyme known to associate with 26 proteasomes. The carboxyl-terminal regions containing KEKE motifs of both hRpn13 and UCH37 are involved in their physical interaction. Knockdown of hRpn13 caused no obvious proteolytic defect but loss of UCH37 proteins and decrease in deubiquitinating activity of 26S proteasomes. Our results indicate that hRpn13 is essential for the activity of UCH37.

The EMBO Journal (2006) **25**, 4524–4536. doi:10.1038/sj.emboj.7601338; Published online 21 September 2006
Subject Categories: proteins
Keywords: deubiquitinating enzyme; proteasome; Rpn13; ubiquitin; UCH37

Introduction

The ubiquitin–proteasome system is the main non-lysosomal route for intracellular protein degradation in eukaryotes (Glickman and Ciechanover, 2002). Short-lived proteins as well as abnormal proteins in cells are recognized by the ubiquitin system and are marked with ubiquitin chains as a degradation signal. Polyubiquitinated proteins are then recognized and degraded by 26S proteasomes. The 26S proteasome is a huge protein complex of approximately 2.5 MDa composed of one proteolytically active 20S proteasome and two 19S regulatory particles (RP), each attached to one end of the 20S proteasome (Baumeister *et al*, 1998). The 20S proteasome is a barrel-shaped complex formed by the axial stacking of four rings made up of two outer α-rings and two inner β-rings, which are each made up of seven structurally similar α- and β-subunits, respectively, being associated in the order of $\alpha_{1-7}\beta_{1-7}\beta_{1-7}\alpha_{1-7}$ (Coux *et al*, 1996). The interior of the cavity composed of β-rings is responsible for its proteolytic activity. However, the entry of substrates into the cavity of 20S proteasomes is restricted by the narrow gate of α-rings, which is closed in itself. The 19S RP plays an important role in the degradation of ubiquitinated proteins. The 19S RP can be divided into two subcomplexes, known as 'base' and 'lid' (Glickman *et al*, 1998). The base is made up of six ATPases (Rpt1–Rpt6) and two large regulatory components, Rpn1 and Rpn2, functioning as presumptive receptor(s) of ubiquitin-like proteins (Leggett *et al*, 2002), whereas the lid contains multiple non-ATPase subunits (Rpn3, Rpn5–9, Rpn11–13, and Rpn15). The base complex binds to the outer α-ring of the 20S proteasome and opens a narrow gate in an ATP-dependent manner (Smith *et al*, 2005). In addition, the ATPase subunits supply energy for unfolding target proteins, so that they can be translocated into the β-ring cavity of 20S proteasomes where active sites are located. The role of the lid complex is less unraveled. Among the lid subunits, Rpn11 is known as a metalloprotease that cleaves the peptide bonds between the substrate and the most proximal ubiquitin of the polyubiquitin chains (Verma *et al*, 2002; Yao and Cohen, 2002). Rpn10 is thought to lie between the base and the lid complex and serve as one of the ubiquitin receptors (Verma *et al*, 2004).

In addition to the genuine proteasome subunits, several molecules that associate with proteasomes and play auxiliary roles have been identified (Verma *et al*, 2000; Leggett *et al*, 2002). Most of the proteasome studies have been carried out using yeast cells, especially budding yeasts, and less is known about mammalian proteasomes and some of the counterparts of yeast proteasome subunits have not yet been identified. Here, we show that Adrm1, which was previously reported as a membrane glycoprotein (Shimada *et al*, 1991, 1994), is an ortholog of yeast Rpn13 and identify it as a novel interacting protein of mammalian 26S proteasomes. Furthermore, we reveal that it recruits UCH37, a deubiquitinating enzyme (DUB) associated with proteasomes (Lam *et al*, 1997; Li *et al*, 2000; Stone *et al*, 2004).

Results

Adrm1 is a mammalian ortholog of yeast Rpn13

To identify proteins involved with mammalian proteasomes, we searched for cellular proteins that physically associate,

*Corresponding author. Laboratory of Frontier Science, Core Technology and Research Center, Tokyo Metropolitan Institute of Medical Science, 3-18-22 Honkomagome, Bunkyko-ku, Tokyo 113-9613, Japan. Tel./Fax: +81 3 3823 2237; E-mail: smurata@rinshoken.or.jp

Received: 21 February 2006; accepted: 15 August 2006; published online: 21 September 2006

directly or indirectly, with 26S proteasomes in mammalian cells. For this purpose, the human ortholog of Rpn10 (hRpn10: hereafter, 'h' is used as a prefix to indicate a human ortholog of any yeast proteasome subunit) with a carboxyl-terminal Flag tag was expressed in HEK293 cells and immunoprecipitated from cell lysates with anti-Flag antibody. The immunoprecipitates were eluted with Flag peptides, digested with Lys-C endopeptidase, and analyzed using a highly sensitive direct nano-flow liquid chromatography/tandem mass spectrometry (LC–MS/MS) (Natsume *et al*, 2002). Following a database search, 30 peptides were assigned to MS/MS spectra for Flag-hRpn10-associated complexes (Supplementary Figure 1). These data identified almost all the subunits of 26S proteasomes. In addition, we identified a molecule with yet unknown relevance to proteasomes, called Adrm1.

Adrm1 was previously reported as a membrane glycoprotein with a molecular mass of 110 kDa and involved in cell adhesion (Shimada *et al*, 1994; Simins *et al*, 1999; Natsume *et al*, 2002). Exploration of the Proteome BioKnowledge Library (https://www.proteome.com/proteome/Retriever/index.html) database indicated that Adrm1 is weakly homologous to Rpn13, a subunit of budding yeast proteasomes (Verma *et al*, 2000). The overall sequence of Adrm1 showed 24.9% homology with that of Rpn13, whereas it exhibited a high homology of 60.2% with the amino-termini of Adrm1 (residues 22–111) and Rpn13 (residues 7–103). We also identified 74.4% homology between the C-termini of Adrm1 (residues 366–407) and Rpn13 (residues 114–156) (Figure 1). Accordingly, we renamed the molecule hRpn13.

Identification of hRpn13 as a novel proteasome interacting protein in mammals

To verify that hRpn13 is a human counterpart of yeast Rpn13, we tested whether hRpn13 is incorporated into 26S proteasomes. Extracts of 293T cells were fractionated by glycerol gradient centrifugation, and each fraction was subjected to immunoblotting with anti-hRpn13 antibody. Almost all hRpn13 proteins co-sedimented with 26S proteasomes that were detected by succinyl-Leu-Leu-Val-Tyr-7-amido-4-methylcoumarin (Suc-LLVY-MCA)-hydrolyzing activity and sedimentation of a genuine proteasome subunit hRpn1 (Figure 2A). Free forms of hRpn13 were not apparently observed (Figure 2A). 26S proteasomes were further purified from fractions 18–20 by immunoprecipitation using anti-hRpt6 antibody, and then the immunoprecipitates were subjected to two-dimensional polyacrylamide gel electrophoresis (2D-PAGE). Immunoblot for hRpn13 detected a spot that had an isoelectric point (p*I*) and molecular mass that corresponded to the predicted values of p*I* 4.8 and 42.1 kDa, respectively (Figure 2B). Tandem mass spectrometric analysis identified this spot as Adrm1 (data not shown). Adrm1 has been reported as a glycosylated membrane protein with a molecular mass of 110 kDa (Shimada *et al*, 1994), which is in conflict with the notion that Adrm1, that is, hRpn13, is a subunit of proteasomes. Immunostaining of HeLa cells using anti-hRpn13 and anti-hRpn1 antibodies showed that the distribution of hRpn13 was mainly in the nucleus and partially in the cytosol, a pattern quite similar to the distribution of hRpn1 (Figure 2C). These results were in agreement with those reported previously showing that proteasomes are predominantly present in the nuclei of rapidly proliferating mammalian cells (Kumatori *et al*, 1990). Thus, in our hands, there was no evidence that hRpn13 is a membrane protein.

Next, we examined whether all 26S proteasomes contain hRpn13. The 26S proteasome fractions (fractions 18–20 in Figure 2A) were immunodepleted using anti-hRpt6 antibody, anti-hRpn13 antibody, or preimmune serum. Anti-hRpt6 antibody completely immunodepleted hRpn13 and other 19S RP

Figure 1 Sequence alignment of human Adrm1 and budding yeast Rpn13. The amino-acid sequences were aligned by the DIALIGN-T program. Amino acids that are identical, strongly similar, and weakly similar between the two sequences are boxed in black, dark gray, and light gray, respectively. Hs: *Homo sapiens*; Sc: *Saccharomyces cerevisiae*.

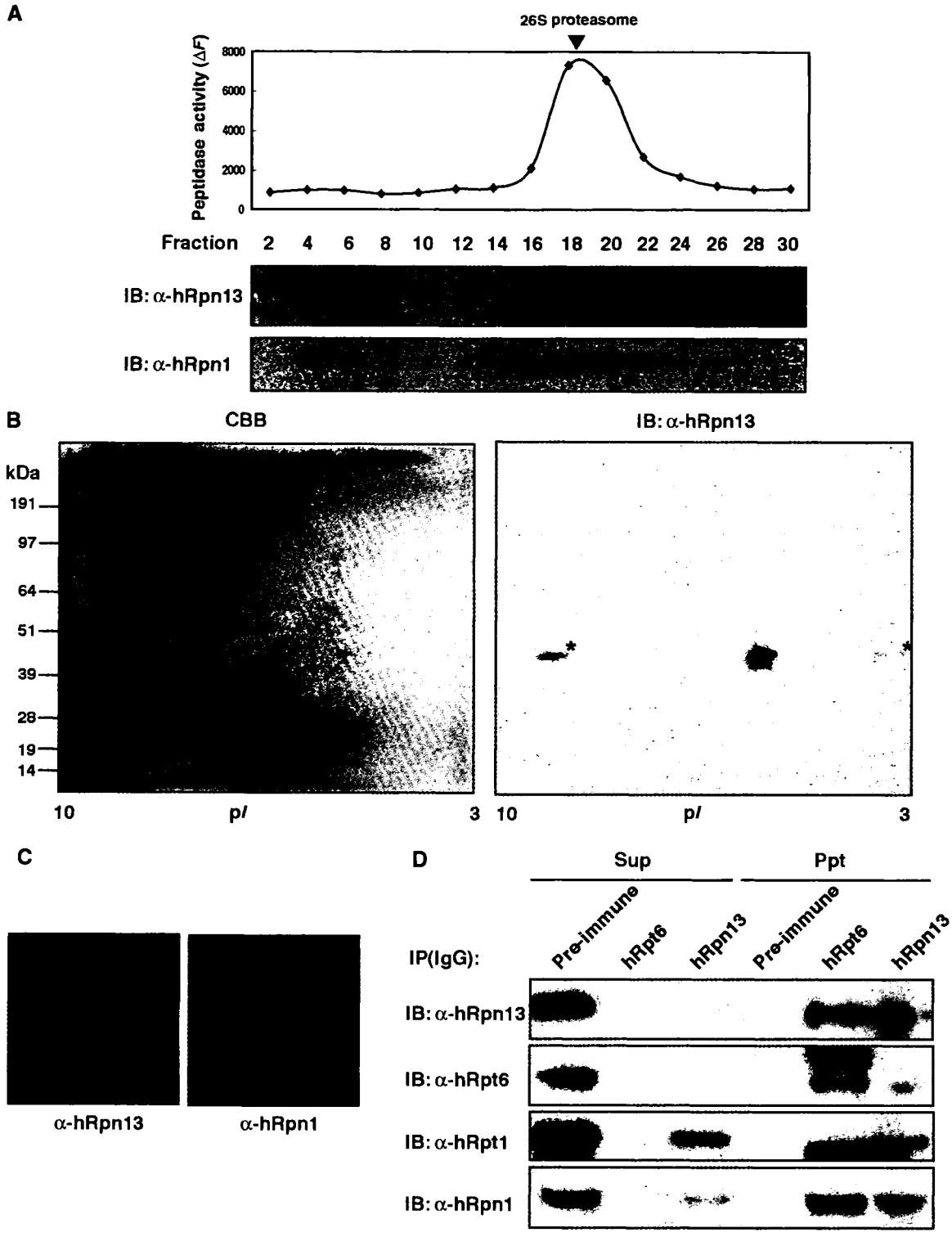

Figure 2 hRpn13 is a subunit of mammalian 26S proteasomes. (**A**) Sedimentation velocity analysis. Extracts of HEK293T cells were fractionated by 10–40% glycerol gradient centrifugation into 32 fractions from the top. An aliquot of each fraction was subjected to the assay of Suc-LLVY-MCA-hydrolyzing activity (upper panel). Immunoblot analysis of each fraction was performed using antibodies against hRpn1 and hRpn13 (lower panels). Arrowhead indicates the peak fraction of 26S proteasomes. Asterisk indicates artifact bands. (**B**) Affinity purification of human proteasomes. Fractions 18–20 in panel A were subjected to immunoprecipitation using anti-hRpt6 antibody. The precipitates were eluted with glycine–HCl and resolved by 2D-PAGE, followed by Coomassie brilliant blue (CBB) staining (left panel) and immunoblot with anti-hRpn13 antibody (right panel). (**C**) Intracellular distribution of hRpn13 in HeLa cells. hRpn13 (left panel) and hRpn1 (right panel) were detected with anti-hRpn13 or anti-hRpn1 antibody and visualized with Alexa488-conjugated anti-rabbit IgG antibody. (**D**) Immunodepletion analysis. Fractions 18–20 in panel A were pooled and immunoprecipitated with anti-hRpt6 antibody, anti-hRpn13 antibody, or preimmune serum. The unbound fractions and immunoprecipitates were subjected to SDS–PAGE, followed by immunoblotting for hRpn13, hRpt6, hRpt1, and hRpn1.

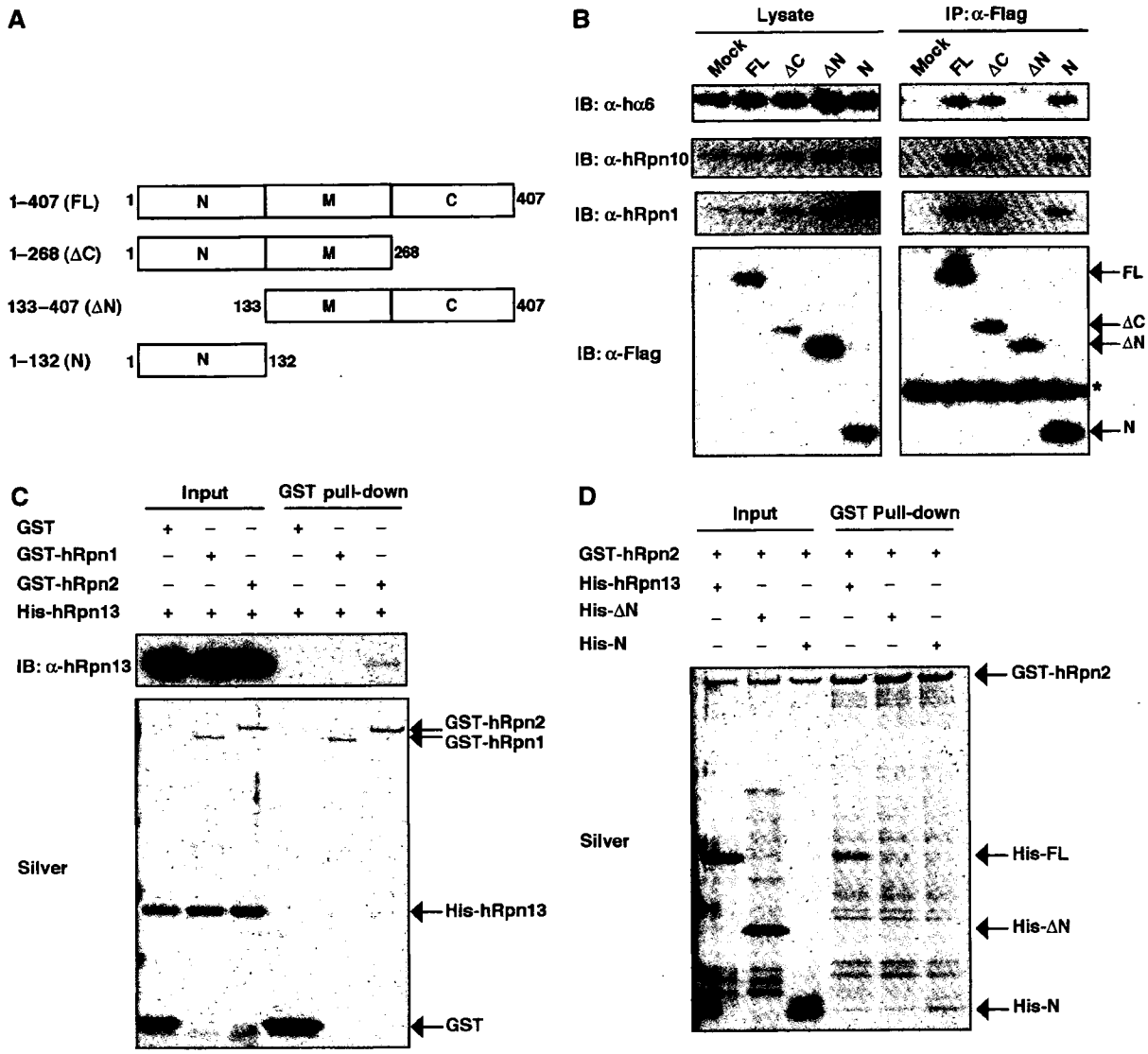

Figure 3 hRpn13 associates with proteasomes via its N-terminal region. (**A**) Schematic representation of constructs for Rpn13 and its dissected mutants used. (**B**) Flag-tagged plasmids encoding hRpn13 and its deletion mutants depicted in panel A were transfected into HEK293T cells. The cell lysates were immunoprecipitated with anti-Flag antibody, followed by immunoblotting for hα6, hRpn10, hRpn1, and Flag epitopes. (**C**) GST pull-down analysis of recombinant proteins. GST, GST-hRpn1, and GST-hRpn2 were incubated with 6xHis-hRpn13 for 1 h at 4°C and then precipitated with glutathione Sepharose. The bound proteins were analyzed by SDS–PAGE, followed by silver staining and immunoblotting with anti-hRpn13 antibody. (**D**) GST pull-down analysis of recombinant proteins. GST-hRpn2 was incubated with 6xHis-hRpn13 or its mutant forms and then pulled down with glutathione Sepharose followed by silver staining.

subunits such as hRpt1 and hRpn1. In contrast, anti-hRpn13 antibody did not remove all the 19S RP subunits, with about 10% input of 19S RP being left in the unbound fraction, whereas it completely depleted hRpn13 (Figure 2D). These results indicate that hRpn13 is incorporated into the majority of 26S proteasomes, but a portion of 26S proteasomes does not contain hRpn13. Therefore, we conclude that hRpn13 is one of the near-stoichiometric proteasome interacting proteins (PIPs), like Ubp6 and Ecm29 in budding yeast (Leggett *et al*, 2002), and is not an integral subunit of 26S proteasomes.

The conserved N-terminal region of hRpn13 is required for association with proteasomes

Based on the sequence alignment, we postulated that hRpn13 is composed of three regions. The N- and C-terminal regions are conserved between budding yeast and human, and the internal region that lies between the N- and C-terminal regions is not found in the budding yeast Rpn13 (Figure 1). We tentatively divided hRpn13 into three portions. The 'N' portion encompassed the conserved N-terminal region (i.e. amino acids 1–132) and the 'C' portion corresponded to amino acids 269–407 that included the conserved C-terminal region. The portion between 'N' and 'C' was designated 'M' portion (Figure 3A). In the next step, we determined the portion required for incorporation into proteasomes. Various deletion constructs encoding wild-type and mutant hRpn13 with Flag tag were expressed in HEK293T cells and immunoprecipitated with anti-Flag antibody. The hRpn13 mutants that lacked the C portion or encoded solely the N portion precipitated various proteasome subunits such as hα6, hRpn10, and hRpn1, as did full-length hRpn13 (Figure 3B). In contrast, hRpn13 that lacked the N portion did not precipitate these subunits (Figure 3B). These results indicate

that the N portion, that is, the conserved N-terminal region of hRpn13, is essential and sufficient for its association with proteasomes.

hRpn13 directly interacts with a base subunit hRpn2

The next set of experiments determined the subunit of 26S proteasomes associated with hRpn13. For this purpose, we tested the interaction between hRpn13 and each subunit of mammalian 19S RP by yeast two-hybrid analysis. The results identified hRpn1 and hRpn2 as possible interacting subunits with hRpn13 (data not shown). Furthermore, comprehensive interactive proteome analysis in budding yeast showed interaction of Rpn13 with Rpn2 (Ito *et al*, 2001). Therefore, we purified recombinant proteins of hRpn1, hRpn2, and hRpn13 and performed *in vitro* binding analysis (Figure 3C). hRpn13 was pulled down by glutathione *S*-transferase (GST)-hRpn2 but not by GST-hRpn1, indicating that hRpn13 is directly associated with hRpn2. Next, we tested whether the N-terminal region of hRpn13 is required for the association with hRpn2. As shown in Figure 3D, the N portion of hRpn13 was required and sufficient for interaction with GST-hRpn2, which was consistent with the results shown in Figure 3B. Based on these results, we conclude that hRpn13 is associated with 26S proteasomes via hRpn2, with which the conserved N-terminal region of hRpn13 interacts.

Knockdown of Rpn13 does not cause proteolytic defects in proteasomes

In budding yeast, deletion of Rpn13 is not lethal, unlike most other proteasome subunits, but causes defect in the degradation of a ubiquitin-fusion-degradation (UFD) substrate (Verma *et al*, 2000). To elucidate the function of hRpn13 in mammalian cells, we knocked down hRpn13 by small interfering RNA (siRNA) in HEK293T cells. As a positive control for proteasome dysfunction, knockdown of hRpt2 was also performed. In hRpt2 knockdown cells, a decrease in hRpt2 protein levels resulted in a concomitant loss of hRpn13 as well as other genuine proteasome subunits such as hRpn1 and hα6. Consequently, hRpt2-knockdown cells showed cell death (data not shown) and accumulation of polyubiquitinated proteins (Figure 4A), which are hallmarks of proteasome dysfunction. These results indicate that hRpt2 is required for the integrity of proteasome structure and function and that hRpn13 is stably expressed in the presence of normal proteasomes. In hRpn13-knockdown cells, the expression of hRpn13 was almost abrogated, but the expression of other proteasome subunits was not changed (Figure 4A). The cells showed normal growth (data not shown) and no accumulation of polyubiquitinated proteins (Figure 4A). These features were in contrast to the phenotypes of hRpt2 knockdown. When the extracts from HEK293T cells were fractionated by glycerol-density gradient centrifugation, an active enzyme that catalyzes the degradation of the fluorogenic substrate Suc-LLVY-AMC was sedimented with a sedimentation coefficient of approximately that of 26S, but low activity was found in the slowly sedimenting fractions corresponding to the sedimentation position of the purified 20S proteasome (Figure 4B, upper panel). The addition of 0.05% SDS, which is a potent artificial activator of the latent 20S proteasome, caused marked activation of the enzyme sedimenting like the 20S proteasome (Figure 4B, lower panel). As shown in Figure 4B, the peptide-hydrolyzing activities of both 20S and 26S proteasomes remained unchanged irrespective of hRpn13 knockdown. Next, we tested the activities of protein degradation *in vitro* (Figure 4C and D) and *in vivo* (Figure 4E). Assay of antizyme (AZ)-dependent ornithine decarboxylase (ODC) degradation, which measures ATP-dependent and ubiquitin-independent proteolytic activity of 26S proteasomes (Murakami *et al*, 1992), did not show decreased proteolytic activity. Rather, the activity was increased 1.4-fold in the hRpn13-knockdown cells (Figure 4C). We also examined ubiquitin-dependent proteolytic activity using *in vitro* ubiquitinated cIAP1 (inhibitor of apoptosis-1), which is a ubiquitin ligase that catalyzes its own ubiquitination for degradation (Yang *et al*, 2000). As shown in Figure 4D, extracts of hRpn13-knockdown cells showed normal proteolytic activity in the degradation of ubiquitinated cIAP1 proteins. IκBα is also a well-known substrate of 26S proteasomes that is rapidly ubiquitinated and degraded in response to TNF-α (Suzuki *et al*, 2000). To check proteasome activities *in vivo*, we monitored the degradation rate of IκBα. hRpn13-knockdown cells showed the same degradation efficiency as control cells (Figure 4E). Considered together, the above results suggest that hRpn13 is not essential for overall protein degradation and viability of mammalian cells.

hRpn13 interacts with UCH37 via its C-terminus

Whereas the N-terminal region of hRpn13 is essential for association with 26S proteasomes (Figure 3), the role of the conserved C-terminal region is still unknown. To elucidate its role, we again used the proteomic approach. Flag-tagged hRpn13ΔN that did not interact with proteasomes (Figure 3) was expressed in HEK293 cells and immunoprecipitated from the cell lysate with anti-Flag antibody, followed by LC–MS/MS analysis. The peptides most abundantly identified were those of UCH37 (also called UCHL5) (Figure 5A), which is reported to be associated with proteasomes in fission yeast, fly, and mammals (Lam *et al*, 1997; Holzl *et al*, 2000; Li *et al*, 2000, 2001; Stone *et al*, 2004). We noticed that both hRpn13 and UCH37 had KEKE motifs at their C-terminal extremities. The conserved C-terminal region of hRpn13 is composed of one typical KEKE at its C-terminus (hereafter referred to as KE2) and one KE-rich region adjacent to KE2, which does not fit the definition of KEKE motif, as proposed previously (Realini *et al*, 1994), but is rich in lysine and glutamic acid residues (hereafter referred to as KE1) (Figure 5B, left panel). A proline residue known as a potent α-helical and β-sheet structure breaker (MacArthur and Thornton, 1991) was located between KE1 and KE2. KEKE motifs are known to mediate protein–protein interactions (Realini *et al*, 1994), and we hypothesized that the interaction between these two molecules was KEKE motif dependent. To test this notion, we expressed Flag-tagged hRpn13, hRpn13ΔKE2 lacking typical KEKE motif, and hRpn13ΔKE1 + 2, which lacked both KE1 and KE2 and thus the entire conserved C-terminal region, in HEK293T cells and immunoprecipitation was achieved with anti-Flag antibody (Figure 5B, right panel). Although the three constructs precipitated nearly the same amount of hα6 and hRpn1, hRpn13ΔKE2 precipitated less amount of UCH37 compared with the wild-type hRpn13, and hRpn13ΔKE1 + 2 did not precipitate UCH37. These results indicate that the conserved C-terminal region is required for the interaction with UHC37.

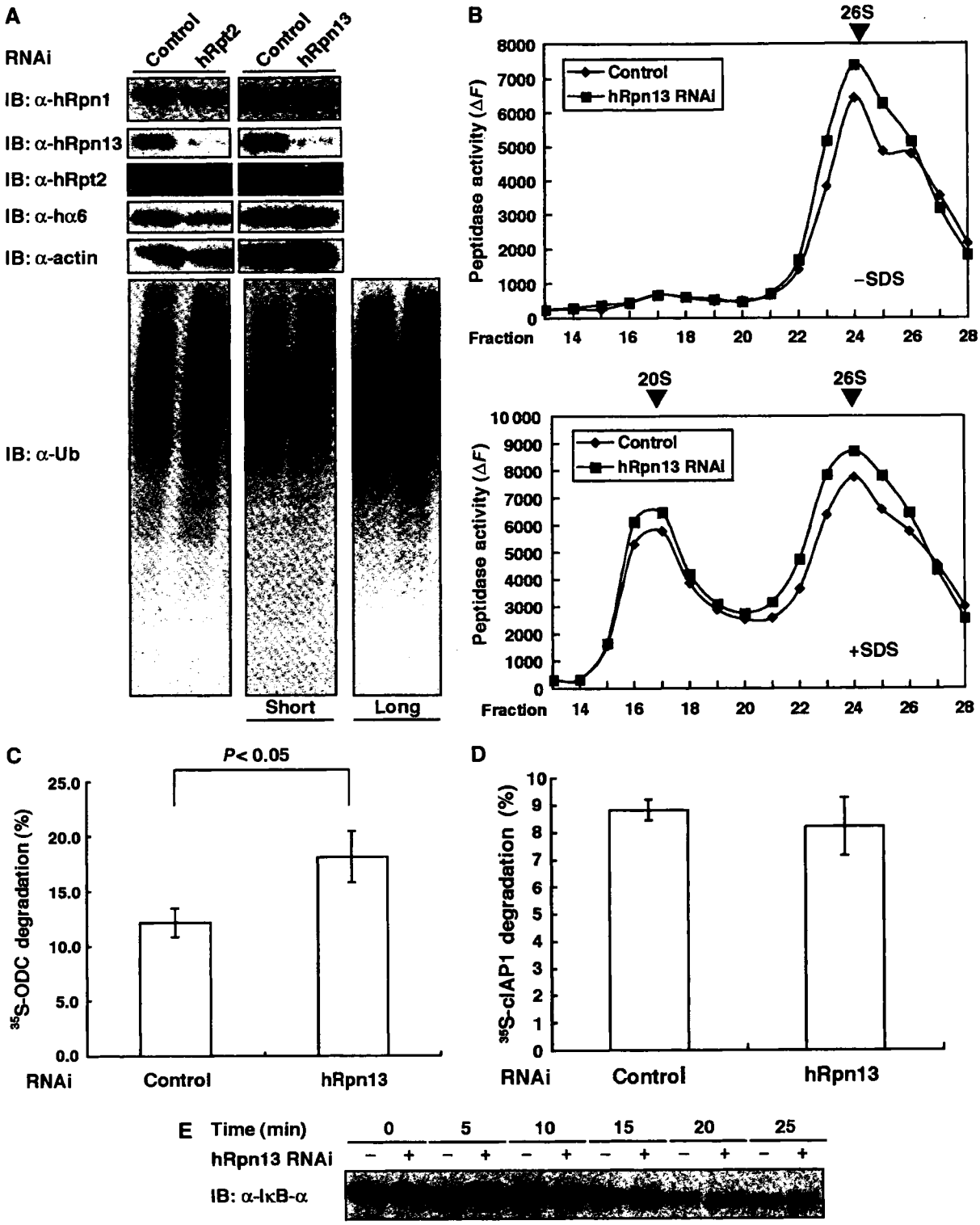

Figure 4 siRNA-mediated knockdown of hRpn13 does not cause proteolytic defects in proteasomes. (**A**) HEK293T cells were transfected with siRNA against hRpn13 or hRpt2. After 48 h for hRpt2 knockdown and 96 h for hRpn13 knockdown, cell extracts were subjected to SDS–PAGE, followed by immunoblotting with the indicated antibodies. (**B**) Extracts of control and Rpn13-knockdown cells were fractionated by 8–32% glycerol gradient centrifugation into 32 fractions from the top. Suc-LLVY-AMC hydrolysis activities were measured in the absence (left) or presence (right) of 0.05% SDS. 20S: 20S proteasome; 26S: 26S proteasome. (**C**) Ubiquitin-independent protein-degrading activity of proteasome. ATP- and AZ-dependent degradation of ^{35}S-labeled ODC protein was assayed. Knockdown cells showed significantly increased activity ($P<0.05$, one-way analysis of variance). Data are mean ± s.e.m. values of three independent experiments. (**D**) Ubiquitinated cIAP1-degrading activity of proteasomes. Ubiquitin-dependent degradation of ubiquitinated ^{35}S-labeled cIAP1 was assayed. Data are mean ± s.e.m. values of three independent experiments. (**E**) Effect of hRpn13 knockdown on TNF-α-induced degradation of IκBα *in vivo*. HEK293T cells were treated with TNF-α for the indicated times in the presence of cycloheximide. The levels of IκBα proteins were analyzed by immunoblotting.

A

Protein symbol	Protein name	Peptides
UCH37	Ubiquitin carboxy-terminal hydrolase 37	7
TIMM13	Translocase of inner mitochondrial membrane 13 homolog	4
YWHAE	14-3-3 epsilon	4
PRDX1	Peroxiredoxin 1	2
USMG5	Upregulated during skeletal muscle growth 5	2
BUB3	BUB3 budding uninhibited by benzimidazoles 3 homolog	1
TIMM8A	Translocase of inner mitochondrial membrane 8 homolog A	1

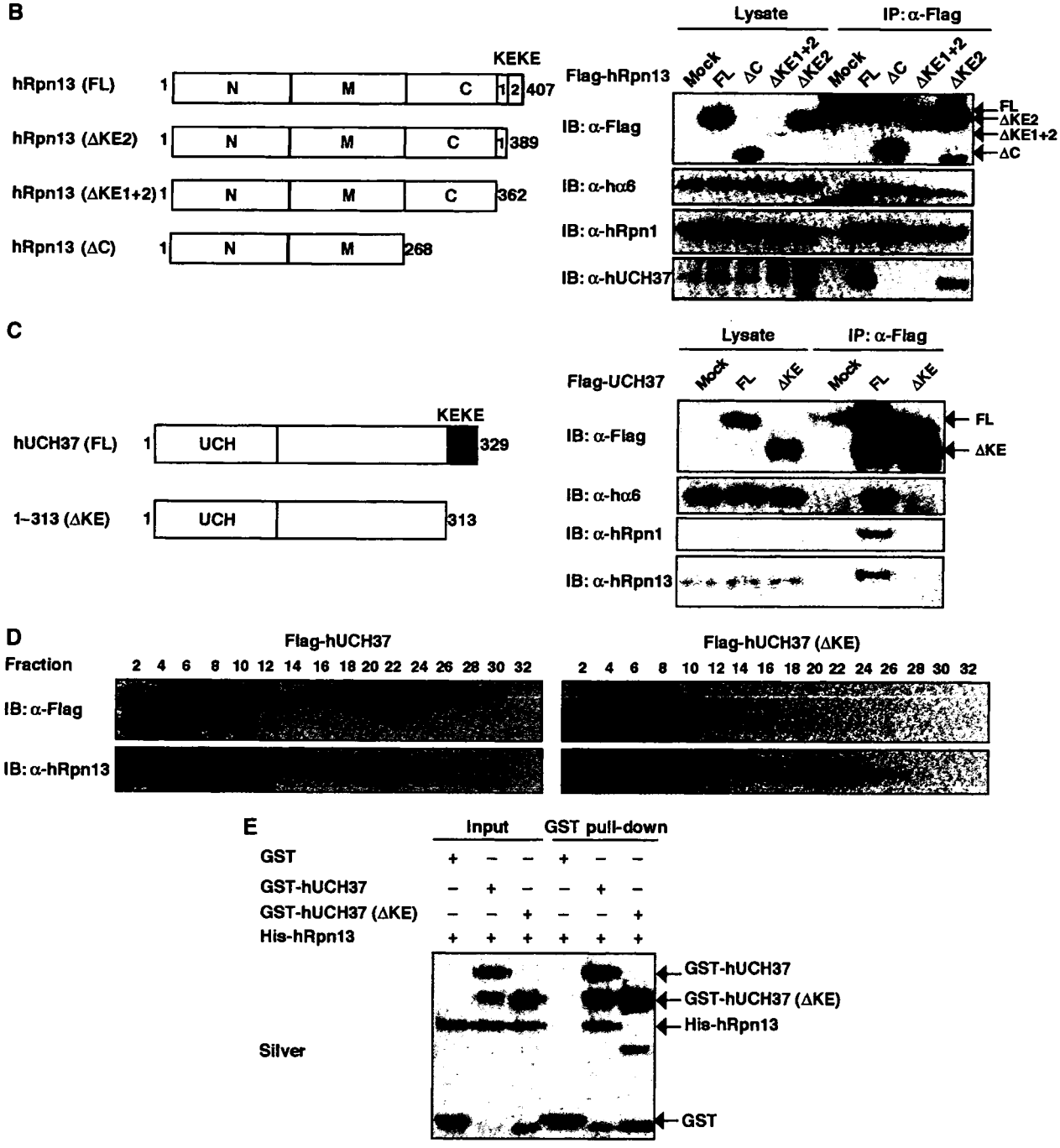

Figure 5 UCH37 interacts with hRpn13. (**A**) A list of proteins detected in four independent hRpn13ΔN immunoprecipitations by LC–MS/MS analysis. The number of identified peptides of each protein is shown. (**B**) Flag-tagged plasmids encoding hRpn13 and its deletion mutants depicted in the left panel were transfected into HEK293T cells. The cell lysates were immunoprecipitated with anti-Flag antibody, followed by immunoblotting for hα6, UCH37, hRpn1, and Flag (right panel). (**C**) Schematic representation of the structures of wild-type UCH37 (FL) and KEKE domain deletion mutant (left panel). HEK293T cells stably expressing Flag-tagged UCH37 (FL), ΔKE, and an empty vector were lysed and subjected to immunoprecipitation with anti-Flag antibody, followed by immunoblot for Flag, hα6, hRpn1, and hRpn13 (right panel). (**D**) The extracts of cells stably expressing Flag-UCH37 and Flag-UCH37ΔKE were fractionated by 10–40% glycerol gradient centrifugation. Immunoblot analysis was performed for each fraction using antibodies against Flag and hRpn13. Asterisks indicate artifact bands. (**E**) GST pull-down analysis of recombinant proteins. GST, GST-UCH37, or GST-ΔKEKE were incubated with 6xHis-Rpn13 and precipitated as in Figure 3C, followed by silver staining.

Next, we examined the role of the KEKE motif of UCH37. As shown in Figure 5C, UCH37 that lacked the KEKE motif (UCH37ΔKE) did not associate with hRpn13 and other proteasome subunits, whereas full-length UCH37 did. Glycerol-density gradient analysis of the extracts showed that a large portion of full-length UCH37 co-sedimented with 26S proteasomes, whereas UCH37ΔKE was observed exclusively in much lighter fractions, presumably as a free form, and that overexpression of UCH37ΔKE did not affect the association of hRpn13 with 26S proteasomes (Figure 5D). In *in vitro* experiments, GST-UCH37 pulled down hRpn13, but GST-UCH37ΔKE did not (Figure 5E), verifying the results depicted in Figure 5C and D. These results indicate that the KEKE motif of UCH37 is necessary for interaction with hRpn13, and hence, with 26S proteasomes.

Knockdown of hRpn13 causes loss of UCH37 proteins

Next, we examined the relationship between hRpn13 and UCH37 in knockdown experiments. We also performed knockdown of USP14, a human ortholog of yeast Ubp6, which is another proteasome-associated DUB (Leggett *et al*, 2002), to examine the relative contributions of UCH37 and USP14 in deubiquitinating activities of 26S proteasomes. Intriguingly, knockdown of hRpn13 caused marked reduction of total cellular UCH37 proteins but not USP14 proteins. On the other hand, knockdown of UCH37 did not affect the level of hRpn13 proteins (Figure 6A). The observed phenotypes of UCH37 knockdown were similar to those of hRpn13 knockdown with regard to cell growth and levels of polyubiquitinated proteins, which were almost the same as the control (Figure 6B and C). Glycerol-density gradient analysis of the extracts of hRpn13-knockdown cells again showed loss of UCH37 proteins in both free and 26S proteasome fractions, with unchanged distributions of proteasome subunits such as hRpn1 and α6 (Figure 6D). Next, we examined the mechanism of decrease in UCH37 proteins in hRpn13-knockdown cells. Control and hRpn13-knockdown cells were treated with various protease inhibitors such as epoxomycin, which is highly specific for proteasomes, MG132, which inhibits both proteasomes and lysosomal enzymes, and E-64d and pepstatin A, which are specific to lysosomal cathepsins. Although these agents worked effectively in inhibiting the relevant proteases (as monitored by the accumulation of polyubiquitinated proteins for proteasome inhibition and accumulation of lipid-conjugated forms of LC3 proteins for inhibition of lysosomal enzymes; Komatsu *et al*, 2005), UCH37 was not increased by any of the inhibitors (Figure 6E). Pulse–chase experiments using HEK293T cells that stably expressed Flag-tagged UCH37 showed almost the same half-life of UCH37 proteins in knockdown cells and control cells (Figure 6F). Semiquantitative reverse transcription–polymerase chain reaction (RT–PCR) showed almost the same expression levels of UCH37 mRNA in hRpn13-knockdown cells and control cells (Figure 6G). Considered together, these results indicate that hRpn13 is required for maintaining normal protein levels of UCH37, and that loss of UCH37 proteins in hRpn13 is not due to metabolic instability of UCH37 proteins or due to repression of transcription of UCH37 mRNA. At present, the mechanism is not clear.

Knockdown of hRpn13 decreases deubiquitinating activities of 26S proteasomes

Finally, we tested the deubiquitinating activities of knockdown cells shown in Figure 6A. As there are abundant DUBs that are not associated with proteasomes, we partially purified complexes of 26S proteasomes and proteasome-associated DUBs by glycerol-density gradient centrifugation, and the 26S proteasome fractions identified by Suc-LLVY-MCA-hydrolyzing activities were used in the following experiments. As shown in Figure 7A, the 26S proteasome fraction of each knockdown cell contained proteasome subunits at a comparable level to each other. Proteins of hRpn13, UCH37, and USP14 were almost completely lost in 26S proteasomes of the cells transfected with siRNAs against hRpn13, UCH37, and USP14, respectively. The deubiquitinating activities of these samples were assayed using ubiquitin-AMC as a substrate. Notably, the deubiquitinating activities of hRpn13- and UCH37-deficient proteasomes were approximately only one-third of those of the control. In contrast, knockdown of USP14 did not significantly reduce the activity. Concomitant knockdown of USP14 with knockdown of hRpn13 or UCH37 did not have additive effects. These results clearly indicate that UCH37 is the dominant DUB associated with mammalian 26S proteasomes and that recruitment of UCH37 by hRpn13 is required for this activity.

Discussion

Adrm1 was originally described as a heavily glycosylated membrane protein of molecular mass 110 kDa (Shimada *et al*, 1991). However, recent studies showed that Adrm1 was hardly, if any, glycosylated and most of it could be detected as a 42 kDa protein (Simins *et al*, 1999; Hasegawa *et al*, 2001; Lamerant and Kieda, 2005). Likewise, the antibody against Adrm1 we raised in this report did not detect the 110 kDa form of Adrm1. Moreover, immunocytochemical analysis of HeLa cells using this antibody indicated that Adrm1 is a soluble protein distributed both in the cytosol and nucleus, which is quite similar to the distribution of proteasomes, as revealed by staining for hRpn1 (Figure 1). Database search analysis suggested that Adrm1 is a human ortholog of yeast Rpn13 subunit. Indeed, Adrm1 was identified in the purified 26S proteasomes at nearly stoichiometric amount, and so we designated it hRpn13. While this manuscript was in preparation, Jorgensen *et al* (2006) reported Adrm1 as a novel proteasome-associated factor (Jorgensen *et al*, 2006). We also identified hRpn2 as an hRpn13-interacting subunit (Figure 3). A previous report mapped the location of p37A (*Drosophila* ortholog of UCH37) in *Drosophila* 26S proteasomes to the interface between the base and the lid, by electron microscopy using gold-labeled ubiquitin-aldehyde bound to the p37A/UCH37 (Holzl *et al*, 2000), which is consistent with our results.

However, immunodepletion analysis showed that not all the 26S proteasomes contain hRpn13 (Figure 2D). In this regard, it is better not to call hRpn13 a subunit of proteasomes but rather regard it as one of the PIPs. Even in yeast, there is no definite evidence to indicate that Rpn13 is a constitutive subunit of proteasomes. In a quantitative mass spectrometric analysis of budding yeast 26S proteasomes, Rpn13 was identified by much smaller number of peptides, compared to authentic proteasome subunits (Guerrero *et al*,